



Nano Scale Disruptive Silicon-Plasmonic Platform for Chip-to-Chip Interconnection

Third Intermediate Progress Report

Deliverable no.: 1.5b
Due date: 15/10/2014
Actual Submission date: 15/10/2014
Authors: KIT, ICMV, TU/e, AIT, UVEG, ST, UGent
Work package(s): WP1-WP7
Distribution level: RE¹
Nature: document, available online in the restricted area of the NAVOLCHI webpage

List of Partners concerned

Partner number	Partner name	Partner short name	Country	Date enter project	Date exit project
1	Karlsruher Institut für Technologie	KIT	Germany	M1	M36
2	INTERUNIVERSITAIR MICRO-ELECTRONICA CENTRUM VZW	IMEC	Belgium	M1	M36
3	TECHNISCHE UNIVERSITEIT EINDHOVEN	TU/e	Netherlands	M1	M36
4	RESEARCH AND EDUCATION LABORATORY IN INFORMATION TECHNOLOGIES	AIT	Greece	M1	M36
5	UNIVERSITAT DE VALENCIA	UVEG	Spain	M1	M36
6	STMICROELECTRONICS SRL	ST	Italy	M1	M36
7	UNIVERSITEIT GENT	UGent	Belgium	M1	M36

¹ **PU** = Public
PP = Restricted to other programme participants (including the Commission Services)
RE = Restricted to a group specified by the consortium (including the Commission Services)
CO = Confidential, only for members of the consortium (including the Commission Services)

Deliverable Responsible

Organization: Karlsruhe Institute of Technology
Contact Person: Martin Sommer
Address: Institute of Microstructure Technology
Hermann-von-Helmholtz-Platz 1, Building 321
76344 Eggenstein-Leopoldshafen
Germany
Phone: +49 (0)721 – 608 22664
Fax: +49 (0)721 – 608 26667
E-mail: martin.sommer@kit.edu

Executive Summary

This document shall incorporate (all) rules procedures concerning the technical and administrative management of the project and is therefore to be updated on a regular basis. Please look at www.navolchi.eu regularly for the latest version.

Change Records

Version	Date	Changes	Author
0.1 (draft)	13/10/2014	Start	Martin Sommer
1 (submission)	15/10/2014		Martin Sommer

INTERMEDIATE PROGRESS REPORT 3

Grant Agreement number: 288869

Project acronym: NAVOLCHI

Project title: Nano Scale Disruptive Silicon-Plasmonic Platform
for Chip-to-Chip Interconnection

Funding Scheme: Collaborative Project

Date of latest version of Annex I against which the assessment will be made:
2014-07-25

Intermediate report: 3rd

Period covered: from 2013-02-01 to 2014-09-30

Name, title and organisation of the scientific representative of the project's coordinator²:

Prof. Dr. Manfred Kohl
Karlsruhe Institute of Technology
Tel: +49-721-608 22798
Fax: +49-721-608 25522
E-mail: manfred.kohl@kit.edu

Project website³ address: www.navolchi.eu

² Usually the contact person of the coordinator as specified in Art. 8.1. of the Grant Agreement.

³ The home page of the website should contain the generic European flag and the FP7 logo which are available in electronic format at the Europa website (logo of the European flag: http://europa.eu/abc/symbols/emblem/index_en.htm logo of the 7th FP: http://ec.europa.eu/research/fp7/index_en.cfm?pg=logos). The area of activity of the project should also be mentioned.

Contents

1	Introduction.....	5
2	NAVOLCHI Summary	6
3	Core of the Report.....	8
3.1	Project Objectives for the Period.....	8
3.2	Work Progress and Achievements	10
3.2.1	Work Package 1: Project Management.....	10
3.2.2	Work Package 2: Interconnect Specifications	10
3.2.3	Work Package 3: Plasmonic Transmitter.....	12
3.2.4	Work Package 4: Plasmonic Receiver	20
3.2.5	Work Package 5: Optical and Electrical Interfaces	29
3.2.6	Work Package 6: Integration, Characterising and Testing	36
3.2.7	Work Package 7: Exploitation and Dissemination	39
3.3	Project Management (Work Package 1).....	45
3.3.1	Request for Amendment	45
3.3.2	Administrative Boards and Decisions.....	45
3.3.3	Management Deliverables.....	46
3.3.4	Communication: Meetings and Phone Conferences	46
3.3.5	New Delivery Dates for Deliverables and Milestones.....	47
3.3.6	Legal Status.....	47
3.3.7	WEB-site.....	47
3.3.8	Management Summary	47
3.4	Deliverables and Milestones Tables.....	49
3.4.1	Deliverables	49
3.4.2	Milestones	51
4	Attachments	54

1 Introduction

The report here present summarizes the results and achievements during month 28 and month 36 of the NAVOLCHI project. This third intermediate report is an additional report exceeding the originally planned list of four major reports during the project:

- First Intermediate Report after 9 months,
- First Periodic Activity Report after 18 months,
- Second Intermediate Report after 27 months and
- Second Periodic Activity Report after 36 months.

Because an extension of the project has been granted by the EC, an additional review becomes necessary which is planned to be held at month 37 (November 2014). As a basis for the review, this report gives an overview over the period from the second intermediate report up to now, i.e. from month 28 up to month 36.

Due to its intermediate' character, this report focuses mainly on the technological and scientific achievements along the report period. Although following the outline of a regular periodic report, some parts have been omitted or changed: Contrary to a periodic report, here the 'Declaration by the scientific representative of the project coordinator' is not needed and the 'Publishable summary' has changed to a simple 'Summary'. Additionally, no finances, no manpower and no FormCs are prepared, because this is necessary for the periodic and final reports only.

2 NAVOLCHI Summary

WP1 (Project Management) Summary

Since the last intermediate progress report, measures have been taken to cope with the retreat of ST from WP6 and delays in technology development.

The ST group responsible for on-chip and off-chip communication (ISG, Interconnect Systems Group) has been closed. As a consequence, the activity and resources of A. Scandurra have been moved to the microcontroller division (MCD) that is not involved in plasmonic devices. However, the Silicon Photonics Group at ST has a continuing interest in the progress and outcome of the Navolchi project. Since they have not the resources to complete the remaining tasks, ST will keep only a limited active role in the development of the final demonstrator (2 MM). Instead, ETH will take over as a new partner to fulfill the remaining tasks (17.5 MM).

A project extension by 9 months has become necessary due to the reorganization at ST and delays in technology development and fabrication of the laser and detector. In particular, the laser is the most disruptive development with the highest risk. Yet, it is considered to be a key component of the envisioned plasmonic interconnect.

By decision of the EC, both aspects have been met with the acceptance of an appropriate amendment to the General Agreement. Consequences are discussed in more detail in Chapter 3.3. With this helpful decision, the outstanding tasks and the contingency plan for the integration, demonstration and performance evaluation of the NAVOLCHI system outlined in the previous intermediate progress report seem to be accomplishable. Details to the technical aspects of the project are given in the corresponding chapters.

WP2 (Interconnect Specifications) Summary

The main effort has focused on the update of the system model according to the final targeted devices within the project. This resulted in significant modifications with respect to the initial model. However, the lack of key parameters from certain devices has delayed significantly the targeted evaluation studies with the developed and updated simulation platform. Some initial work has been conducted on the techno-economical evaluation studies primarily focusing on the required type of data from the device manufacturers for the completion of such studies.

WP3 (Plasmonic Transmitter) Summary

It is the aim of WP3 for the reporting period to carry out the characterization of the individual plasmonic devices comprising the transmitter. Each plasmonic device has been identified to be a challenge by itself, thereby some of the proposed devices have been finalized, while others are expected to be demonstrated during the remaining duration of the project. This report contains the latest characterization information of all individual plasmonic devices within WP3. When no characterization results in terms of device performance are available, characterization in terms of up-to-date fabrication results is provided. In section two, the latest efforts of TUE to fabricate the electrically pumped integrated nanolaser is presented, and then full characterization of the plasmonic modulator developed by KIT, both as a phase modulator and in a Mach-Zehnder configuration is reported. In this report, the device characterization is presented within the fabrication tasks of the project.

WP4 (Plasmonic Receiver) Summary

From previous and new measurements the peak gain of HgTe QDs is of the order of 400 dB/cm for a closed-packed film of this material, indicating that 10 dB gain under optical pumping is feasible. However, results on both closed-packed QD and QDs dispersed on PMMA does not seem to reach such a net gain, possibly because of the HgTe QD photostability. In parallel, the two concepts of hybrid-plasmonic amplifiers incorporating QDs (using polymer and SiN waveguides) have been fabricated and characterized by using CdSe QDs emitting at visible and HgTe QDs emitting at NIR wavelengths. Metal waveguides (planar and ridges) have been fabricated and used to investigate the observed increase of the SPP propagation length by optical pumping of QDs, even if net gain cannot be achieved by the available material.

In the case of photodetectors based on quantum dots important advances have been reached during the last year: i) **reproducible** and optimized conductive films of PbS QDs prepared by Dr. Blasing were achieved along several series of devices, ii) the best value for the responsivity in Schottky-heterostructure photodetector was around **0.16 A/W** at the exciton peak absorption (≈ 1620 nm), iii) the best value of dark current was 70 nA with an ideality factor around 3, using Ag electrodes, iv) at 1550 nm, where $R \approx 0.1$ A/W, pumping light above 6 nW can be detected. Plasmonic photoconductors by considering a plasmonic nano-gap waveguide concept were fabricated in collaboration with TUE-group and are under characterization.

WP5 (Optical and Electrical Interfaces) Summary

WP5 focuses on realizing the optical and electrical interfaces for the plasmonic interconnection platform. Most of the work in this WP has been completed in previous reporting periods: KIT finished the design and fabrication of the interfaces between silicon waveguides and plasmonic modulators while IMEC finished the work on the compact filters. Work in the current period related to the fabrication of the focusing grating couplers (IMEC), which is underway, and to the design and the functional verification of the Dual Die Communication Module (DDCM) compatible with a plasmonics-based physical layer (PHY).

WP6 (Integration, Characterising and Testing) Summary

This work package was under responsibility of ST, which declared to stop work on the work package in the beginning of 2014 (project month 26). According to the decision of the EC, ETH is taking over as a work package leader for the remaining part of the project.

WP7 (Exploitation and Dissemination) Summary

Dissemination and exploitation of ideas and results is of high importance in the project. There is substantial dissemination action concerning project activities. In particular, NAVOLCHI partners have already produced several high quality scientific journal and many conference publications (papers/presentations/talks). The project website (www.navolchi.eu) has been implemented and uploaded online, disseminating the NAVOLCHI activities further. A press release and an advertising brochure have been issued.

On the exploitation front, 1 patent has been submitted successfully, and several Master and PhD theses on NAVOLCHI technology have been initiated at partners' institutes.

3 Core of the Report

3.1 Project Objectives for the Period

WP1 (Project Management) Objectives

Besides the good results obtained in the months before, the consortium faced two major problems around project month 26:

- ST intended to reduce its engagement in work package 6. To overcome this, the Consortium proposed to include ETH as an additional partner of the NAVOLCHI project, who should take over activities of work package 6.
- The Consortium intended to extend the project activities by 9 month due to delays in development of fabrication technology and due to STs reduced engagement in WP6.

The request for amendment containing both subjects was granted by the EC at September 16th 2014.

WP2 (Interconnect Specifications) Objectives

- System modeling update according to latest data from available components and targeted systems
- Identification of design tolerances for the modules under development
- Cost and power consumption evaluation studies

WP3 (Plasmonic Transmitter) Objectives

The main objective of WP3 for the reporting period was to carry out the characterization of the plasmonic transmitter. There are no milestones corresponding to WP3 within this period, however the main characterization results have been reported within WP6. Additionally WP3 has reported D3.3 and D3.4 regarding the fabrication technology of the transmitter devices.

WP4 (Plasmonic Receiver) Objectives

Plasmonic Amplifier:

- IR Quantum Dots (HgTe) with gain.
- Plasmonic Amplifier concept by using polymers incorporating those IR QDs (optical injection).
- Si based Plasmonic Amplifier platform incorporating those IR QDs (optical electrical injection).

Photodetectors using QDs and metal nanostructures

- PbS quantum dots absorbing light at telecom wavelengths and conductive films based on them.
- Photodetectors based on these films reaching responsivities above 0.1 A/W at telecom wavelengths: Schottky/heterostructure vs nanogap/microgap devices.

- Fabrication of nano-gap waveguide photoconductors.

WP5 (Optical and Electrical Interfaces) Objectives

- Fabrication of focusing grating couplers
- Dual Die Communication Module (DDCM) compatible with plasmonics- based PHY design and functional verification
- DDCM evolution for Network in Package (NiP) solutions

WP6 (Integration, Characterising and Testing) Objectives

This work package is under responsibility of ST, which declared to stop work on the work package in the beginning of 2014 (project month 26). According to the decision of the EC, ETH is taking over as a work package leader for the remaining part of the project. The objective of this WP is:

- The characterization and testing of the particular active and passive plasmonic devices.
- Its integration with the plasmonic interconnect modules, representing the physical layer (PHY) of such a communication structure and
- The System in Package characterization and testing

WP7 (Exploitation and Dissemination) Objectives

- Dissemination through paper submission to high quality and high impact scientific journals, magazines and white papers.
- Promotion of the project outputs through the participation in conferences and symposia.
- Organizing workshops/seminars on NAVOLCHI technology.
- Interaction with other EU-funded and national projects.
- Generation of intellectual property (patents portfolio).
- Theses at the partners' institutes on NAVOLCHI technology.
- Provide input to industrial partners based on scenarios of the proposed solutions.
- Maintenance of the project web site which will be used for information and result dissemination purposes.
- Work Progress and Achievements

3.2 Work Progress and Achievements

3.2.1 Work Package 1: Project Management

Please refer to chapter 3.3 for a detailed description of the activities concerning the project management.

3.2.2 Work Package 2: Interconnect Specifications

The active tasks for the current reporting period are T2.2 on the “Modelling of devices and system for communications applications” and T2.4 on the “Techno-economical evaluation and benchmarking” studies.

General status

The main effort has focused on the update of the system model according to the final targeted devices within the project. This resulted in significant modifications with respect to the initial model. However, the lack of key parameters from certain devices has delayed significantly the targeted evaluation studies with the developed and updated simulation platform. Some initial work has been conducted on the techno-economical evaluation studies primarily focusing on the required type of data from the device manufacturers for the completion of such studies.

Task 2.2 Work Progress (Modelling of devices and system for communications applications)

The aim of this task is to provide the device specifications for the novel disruptive plasmonic Si-photonics platform and its application in the chip-to-chip interconnection environment.

The initial simulation platform has been realized with the commercial VPI Photonics software. This platform simulates an end-to-end system that includes: a) the metallo-dielectric laser source, b) a plasmonic Mach-Zehnder modulator c) the channel for chip-to-chip interconnection d) an (optional) amplification stage and e) the plasmonic receiver.

Based on the latest type of plasmonic devices and the considered experimental system tests, the transmitter and receiver parts of the simulation platform have been modified in order to accurately support the evaluation of the following interconnection systems:

- a) A directly modulated laser (DML) - based system in which the data are applied directly on the driving current of the metallo-dielectric laser source omitting the use of the plasmonic MZM
- b) A binary phase shift keying (BPSK) transmitter, utilizing the plasmonic MZM driven by the metallo dielectric laser source in continuous wave (CW) mode and with differential phase shift keying (DPSK) detection based on a passive delay line interferometer (DLI) at the receiver
- c) An intensity modulation transmitter utilizing the MZM and the laser source in CW mode, with direct detection at the receiver

It is noted that the modifications in the simulation platform applied primarily on the DML model, the driving conditions of the MZM for the two different formats and the inclusion of the DPSK detector with the DLI structure.

Although the updated platform for the simulation of the aforementioned systems is complete, a significant number of parameters concerning primarily the laser structure were not possible to be estimated as long as the specific device is under development. This creates a large number of uncertainties for the accurate evaluation of the DML-based system, since the resulted signal shape from this type of transmitter depends strongly on these parameters and affects the final performance evaluation results.

On the other hand, an adequate number of targeted parameters have been provided for the MZM (also being evaluated experimentally). This allows the study of of system configurations b) and c) mentioned above, for given receiver characteristics and types of interconnection medium.

According to the available data, the system characterization work was decided to focus on the evaluation of the end-to-end loss in the system for different design parameters. The analysis of the overall loss as function of various system parameters (like bit-rate and targeted BER level) will determine in turn:

- a) the tolerable insertion losses for the plasmonic MZM device, as function of the interconnection distance
- b) the tolerable noise level (at the receiver and in the case that an amplification stage is required) for certain interconnection lengths, types of medium and insertion losses
- c) other critical design tolerances related with the laser and receiver parameters (remain to be specified by the project's device manufactures and as these are identified during the development process)

Task 2.3 work progress (Value analysis in terms of cost and green aspects [M25-M30])

This Task is in progress. The final characteristics of the implemented plasmonic devices will need to be provided in order to proceed with an accurate value analysis in terms of cost and green aspects.

Task 2.4 work progress Techno-economical evaluation and benchmarking [M24-36])

This Task is in progress. The final characteristics of the implemented plasmonic devices will be used in order to proceed with an accurate techno-economic evaluation and benchmarking. The implemented plasmonic-based architecture will be evaluated and compared against alternative technologies like photonic and electronic interconnects.

Task 2.5 work progress: VHDL modelling of plasmonic interconnect and CMOS interface circuits [M10-M24]

This task has been completed successfully in M24.

3.2.3 Work Package 3: Plasmonic Transmitter

Task 3.3. Fabrication of plasmonic nanolaser

1. Lithography and etching processes

The definition of the nanostructure is carried out by electron-beam lithography (EBL) due to the high resolution required. This is done in three EBL steps as depicted in Figure 3- 1. During the first lithography, the nanopillar is defined. Later, an overlay exposure is needed to define the waveguide and, finally, the grating coupler is defined with another overlay exposure. Three different lithographic masking schemes are used during these EBL steps, which have been discussed in D1.5.

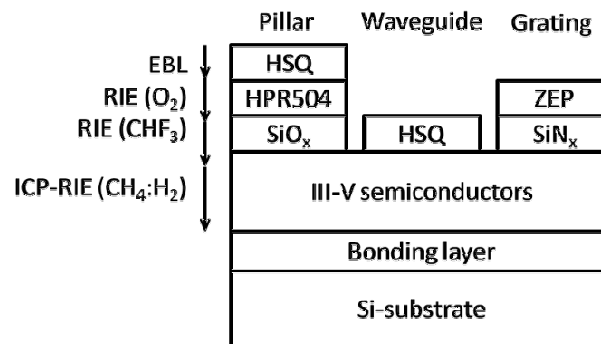


Figure 3- 1: Processing schemes to fabricate the different nanostructures of the laser device.

Using the semiconductor technology developed at TUE and summarized in Figure 3- 1, TUE has been able to fabricate the full semiconductor structure comprising the waveguide-coupled pillar cavity proposed in D3.1. The target laser structure is shown in Figure 3- 2b, whereas a scanning-electron microscope (SEM) picture of the latest outstanding fabrication results is presented in Figure 3- 2a for comparison.

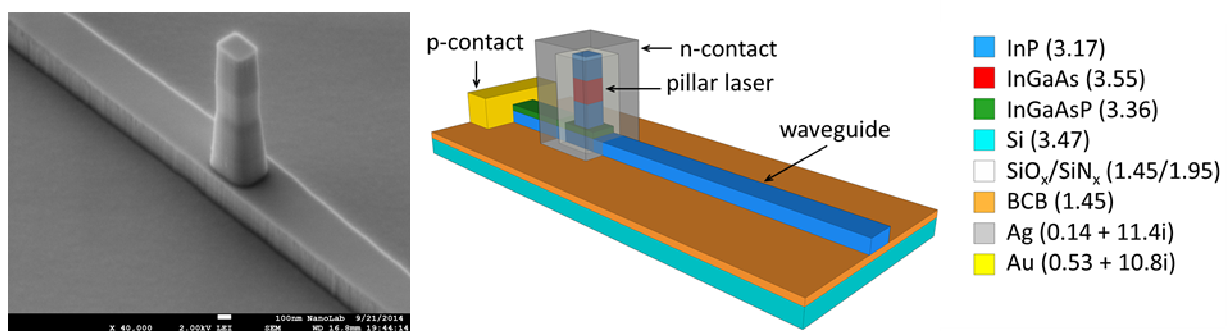


Figure 3- 2: SEM image of the current devices under fabrication. Right: Schematic of the target waveguide-coupled nanolaser.

Results depicted in Figure 3- 2 correspond to a fabrication run under progress in which only the electrical contacts are missing to complete the fabrication. The same metals deposited to fabricate the n-contact will also form the metallic cavity. This run is expected to be completed in November and fully characterized before the end of the year.

2. Low-loss low-contact resistance ohmic contacts

The NAVOLCHI project targets to demonstrate sub-micron size devices. Such small devices allow, in principle, for ultra-low capacitance and therefore ultra-high speed devices as it has already been demonstrated in the plasmonic modulator reported in M14. Nevertheless, as the device size gets smaller, the contact resistance increases drastically, which puts a limitation on the voltage operation point. Therefore progress in electrical contacts is also required to develop fast nanophotonic devices compatible with standard driving electronics.

Due to the importance of the ohmic contacts in active devices, TUE has put efforts into developing suitable ohmic contacts that are compatible with plasmonic devices and provide low electrical and optical loss at the same time. For this, we studied and demonstrated low contact resistance Ge/Ag contacts. Figure 3- 3(left) provides a schematic of the proposed electrical contacts. Since silver itself does not adhere to InP or InGaAs, a thin layer of Germanium is required, which can be as thin as 2 nm according to our experiments. As Germanium has a high refractive index ($n=4.27$ at $1.5 \mu\text{m}$), the use of a thin layer is required to minimize the modal loss due to the strong confinement.

After Ge deposition, silver is deposited by e-beam evaporation and annealed. The annealing step is done to (1) promote silver grain growth to reduce optical loss, and (2) diffuse Ge into the semiconductor layer providing additional doping to decrease the contact resistance. Special care must be taken during this annealing to avoid a deep diffusion which can cause a short circuit in p-i-n structures. Finally, a layer of gold can be sputtered to prevent silver oxidation. The full process can be done using either two lift-off processes, or one lift-off and a metal wet etching.

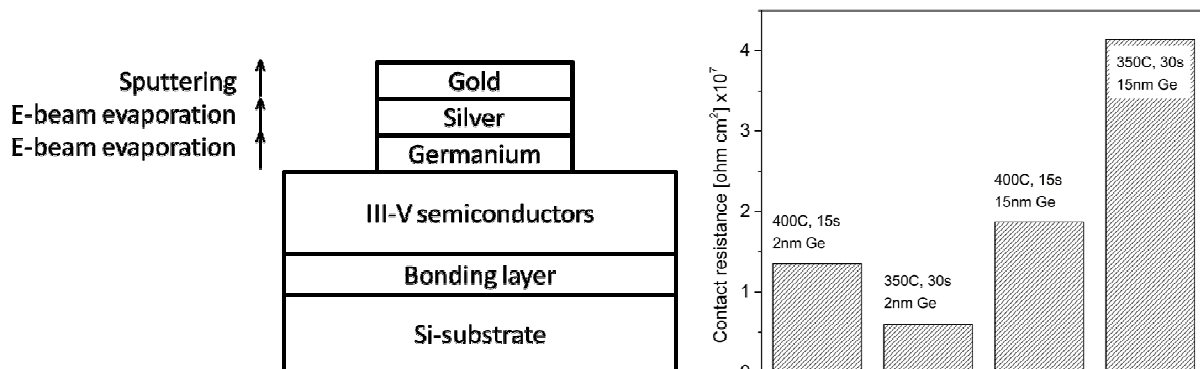


Figure 3- 3: Left: Schematic of Ge/Ag/Au contacts. Right: Characterization of ohmic contacts by the Transmission Line Model on n-InGaAs with doping level of 1×10^{19} .

Experiments with the proposed silver-based contacts were done on n-doped InGaAs, which is the top semiconductor layer of the nano-cavity. The Ge layer was kept as thin as possible (2nm and 15nm), whereas the Rapid Thermal Annealing (RTA) was carried out at 350 °C and 400 °C, with 30 and 15 seconds, respectively. These annealing conditions were previously found to result in silver grain growth in III-V membranes bonded to silicon.

As it can be seen in Figure 3- 3(right), the lowest contact resistance is obtained when using 2 nm Ge and annealing at 350 °C for 30 seconds. In view of the high performance in terms of the contact resistance and the well-known low optical loss of silver, such contacts have been chosen to be implemented in the nanolaser device.

3. Conclusions

The core technology required to fabricate the nanolaser device has been developed at TUE. Different lithography schemes were proposed and successfully demonstrated for the accurate definition of the nano-cavity, waveguide and grating coupler structures. Silver-based ohmic contacts were fabricated and characterized for membrane photonic circuits which showed high performance for the optimum annealing conditions that were earlier found to allow silver grain growth. This fabrication technology is now in the last fabrication run that that is planned to be finished in November and should enable us to demonstrate operating laser devices.

Task 3.4. Fabrication of Si-plasmonic modulators

1. Plasmonic absorption modulator

The plasmonic absorption modulator as described in deliverable 3.4 was characterized in two steps. First, we studied the quasi-static behavior. We measured the current and the optical transmission while slowly sweeping the applied voltage. In a second step, a MHz modulation was applied to the device. In summary, the device shows optical extinction ratios of 12 dB at 1550 nm wavelength for 10 μm long devices. The operation power is below 200 nW with operating voltages in the range of ± 2 V and currents below 100 nA. Tests with 50 write cycles and sinusoidal modulation in the MHz regime demonstrate excellent repeatability of the switching mechanism.

2. Static behaviour

We measured the current and the optical transmission as a function of the applied voltage. The voltage was applied between top and bottom electrode. A compliance current of 100 nA was set to protect the device from permanent breakdown. Continuous wave laser light at a wavelength of 1550 nm was coupled to the chip through grating couplers. The transmitted optical signal was measured with a power meter.

The electrical behavior of a 5 μm long device with the laser being turned off is displayed in Figure 3- 4. The applied voltage was swept from -3 V to 3 V and back in steps of 60 mV with a duration of 2 s per step. We observed a sudden increase of the current at a threshold of ~ 2.9 V. Here, the current reached its compliance limit. When scanning back, the current decreased while showing a hysteresis.

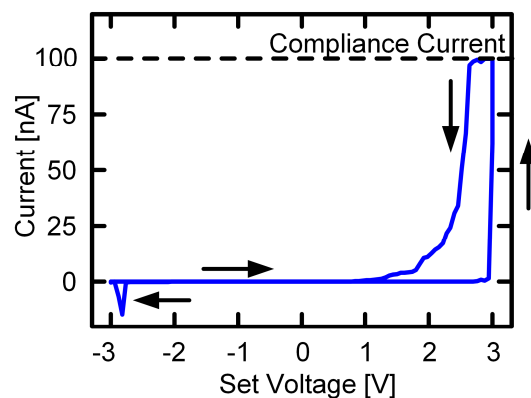


Figure 3- 4: Electrical current-voltage characteristic of the plasmonic absorption modulator. The response indicates a hysteresis. An abrupt increase of the current is found with a threshold around 2.9 V. Note that the set voltage differs from the actual (measured) voltage in the compliance limit.

Figure 3- 5(a) shows the normalized optical transmission for 50 consecutive measurement cycles below threshold (± 2 V, 20 mV per step, 2 s per step, total duration of 13.3 min per cycle). We started at -2 V in the ON state. While gradually increasing the voltage, the optical signal decreased. When decreasing the voltage, the optical transmission increased again, while being lower than for the forward sweep direction. This hysteresis indicates a memory effect of the switch. The device returned to its initial state after completion of each measurement cycle. This shows excellent repeatability of the switching effect. The difference between the ON and the OFF state (extinction ratio) was 6 dB. The latching extinction ratio between the latched states was 3.5 dB. Since the device was operated below threshold, no significant current was measured and no hysteresis was observed in the I-V curve. Therefore, peak operating power during switching is below 200 nW.

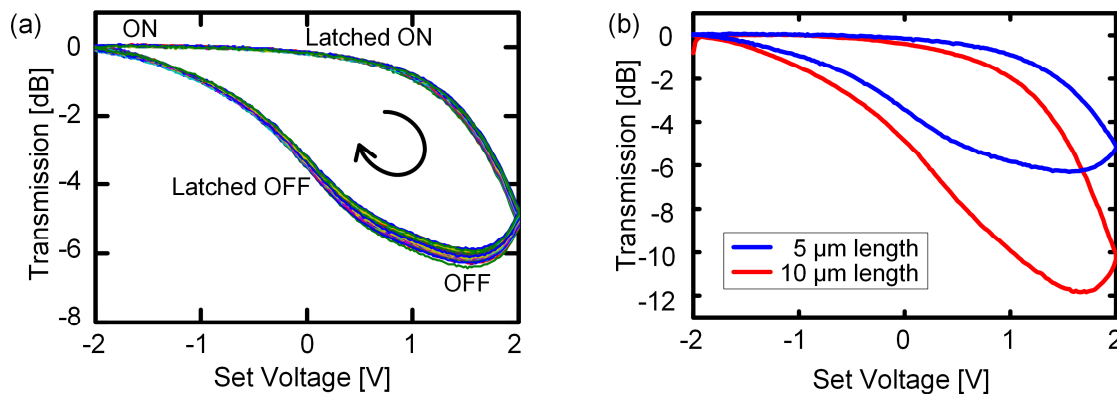


Figure 3- 5: Quasi-static performance of the plasmonic absorption modulator. (a) Latching optical switch behavior for a 5 μm long device: 50 measurement cycles of the normalized optical transmission as a function of the set voltage showing a hysteresis and an extinction ratio of 6 dB. (b) Latching optical switch behavior of a 10 μm long device showing an extinction ratio of 12 dB. During these measurements below threshold, no hysteresis was observed in the I-V curve.

The dependence of the extinction ratio on the device length was investigated as well. From Figure 3- 5(b) one can see that increasing the length from 5 μm to 10 μm increases the extinction ratio from 6 dB to 12 dB. Thus, the extinction ratio increases with increasing device length. While two devices with different lengths do not yet provide sufficient statistics the result at least indicates a trend.

Propagation losses in the hybrid waveguide section of 1 dB/μm and coupling losses between the silicon photonic and the hybrid waveguide of 6.5 dB per interface were determined through cut-back measurements.

2.1. Dynamic behaviour

To further assess the device, we studied the dynamic behavior of the switch. Here, a sinusoidal modulation in the MHz regime was applied to the device and detected with a photodiode and a lock-in amplifier. This revealed a relatively flat frequency response between 40 kHz and 10 MHz. The 3 dB bandwidth at an operation with ± 2 V with respect the amplitude at 40 kHz is 30 MHz (see Figure 3- 6, blue triangles).

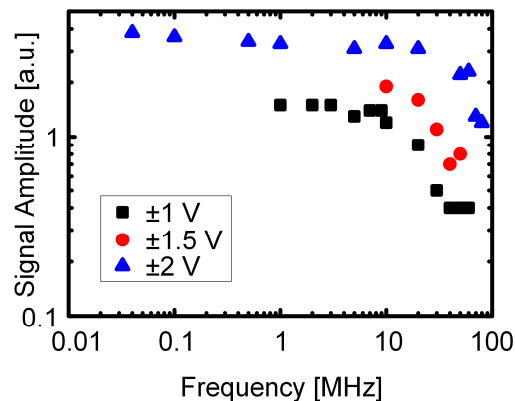


Figure 3- 6: MHz frequency response of the plasmonic absorption modulator. A sinusoidal signal was applied to a 5 μm long device using an arbitrary waveform generator. The optical signal was detected with a photodiode and a lock-in amplifier.

2.2. Plasmonic Mach-Zehnder modulators

The plasmonic Mach-Zehnder modulator consists of two high speed plasmonic phase shifters (see Figure 3- 7(a), Deliverable 3.2 and Deliverable 3.4) placed in the arms of a Mach-Zehnder interferometer realized on a silicon-on-insulator (SOI) wafer. The interferometer is designed with un-balanced arms and the operation point of the modulator is defined by the operating wavelength, see Figure 3- 7(b). Standard photonic multimode interference (MMI) couplers have been used as 3dB optical splitters/combiners. High speed phase modulation is performed by plasmonic phase shifters based on the Pockels effect in an electro-optic (EO) organic material, see Figure 3- 7(a). Applying a voltage between the metal electrodes can change the refractive index of the EO-material due to the Pockels effect, and therefore the phase velocity of the plasmonic mode. The photonic-to-plasmonic mode conversion within the arms of the Mach-Zehnder interferometer is accomplished by the metal taper couplers. Scanning electron microscope image of the active plasmonic phase shifter section is give in Figure 3- 7(c) and Figure 3- 8(a)-(c). To keep the insertion loss of the modulators in the practical range we use low loss silicon MMI with an insertion loss of less than 0.5dB.

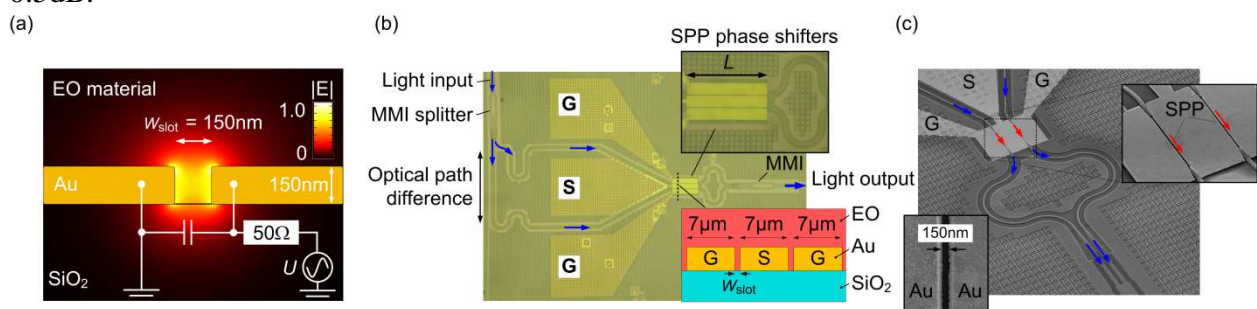


Figure 3- 7: Silicon-plasmonic Mach-Zehnder modulator (MZM) designed and fabricated on a silicon-on-insulator (SOI) platform. (a) Gap surface plasmon polariton (SPP) mode profile in a metal slot filled with an electro-optic (EO) material. The SPP mode is strongly confined to the slot. In addition, a lumped-element equivalent circuit of the modulator is given. Because of the high conductivity of the gold electrodes, the device can be represented by a capacitor ($C_{\text{Device}} \approx 1.5...3 \text{ fF}$, L dependent). (b) Optical microscope image of the fabricated Mach-Zehnder (MZ) modulator. The MZ interferometer is defined on a passive silicon platform, where light splitting / combing is done by low loss photonic multimode interference (MMI) couplers. The photonic to plasmonic mode conversion is accomplished by metal taper couplers. An optical path difference is implemented in the MZ interferometer design to

avoid applying high bias voltages. An optical phase difference between the two arms is modulated by the plasmonic phase shifters. (c) Scanning electron microscope (SEM) picture of the silicon-plasmonic MZM. The modes of the silicon waveguide are coupled to the plasmonic phase shifters, where the phases of the SPPs are modulated. In the end of the phase shifters the SPPs are back converted to photonic modes and then combined within the photonic MMI coupler

The Mach-Zehnder modulators are fabricated on a silicon-on-insulator (SOI) platform with a buried oxide with a thickness of 2 μm , and a silicon device layer with a thickness of 220 nm. First, the passive silicon photonic circuit is fabricated at IMEC, in the frame work of ePIXfab, by using standard processes such as 193 nm DUV lithography and Si dry etching. The plasmonic high-speed phase shifters with a common signal electrode are defined on gold (Au). The metallic slots with the widths of ~ 150 nm slot and the length of 19 μm , 29 μm and 39 μm are defined with e-beam lithography and lift-off process. The slot is filled with an electrooptic material SEO100 (Soluxra, LLC). The electro-optic effect in the EO material is activated through a poling procedure. To avoid electrical breakthroughs, we perform the poling with electrical fields which are lower than the optimum poling field of 100 V/ μm corresponding to the maximum $r_{33} = 110\text{pm/V}$.

2.3. Characterization results of the photonic-to-plasmonic mode converters

We first characterize the photonic-to-plasmonic mode converters using the fabricated test samples consisting of single metallic slot waveguides interfacing to silicon nanowires through two metallic taper mode converts, see Figure 3- 8(a) – (c). By varying the length L_{MSW} of the metallic slot waveguide between the pairs of taper couplers we can extract the conversion efficiency similar to the standard cut-back measurement. Three devices with metallic slot waveguide lengths of L_{MSW} of 1 μm , 29 μm , and 44 μm , see Figure 3- 8(a) – (c). The slot width is about 140 nm for all three cases.

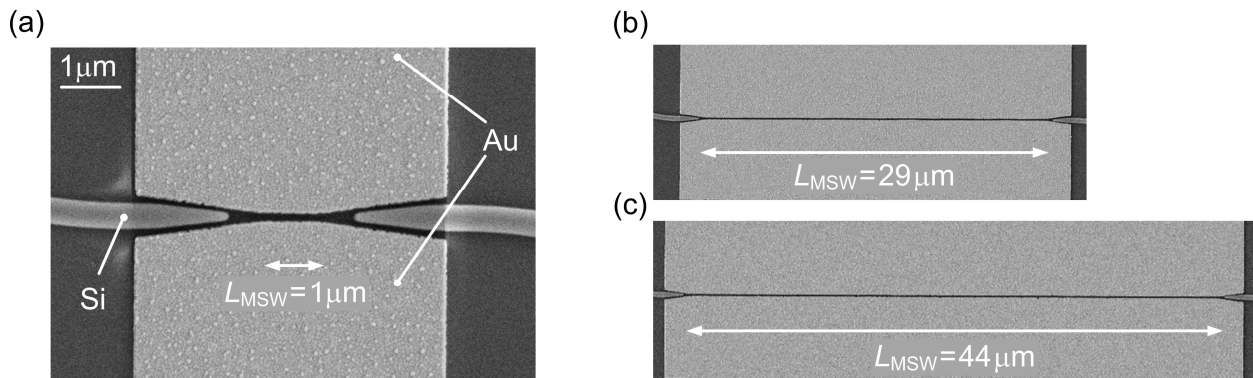


Figure 3- 8: Fabricated metallic tapered mode converters with three different MSW lengths L_{MSW} of (a) 1 μm , (b) 29 μm , and (c) 44 μm . The slot size h is about 140 nm for all three devices.

The measured silicon-to-silicon waveguide transmission spectra for the three different metallic slot waveguide lengths L_{MSW} are given in Figure 3- 9(a). The measured transmission spectra are normalized to the measured reference spectra for a silicon strip waveguide without a plasmonic section. As can be seen, the tapered mode converters exhibit large conversion efficiency in a wide operating wavelength range. A total conversion loss of 1 dB is estimated for two transitions. This is in agreement with the theoretically expected conversion efficiency of 2...3 dB. The difference between theoretically calculated and experimentally measured conversion efficiencies is attributed

to small differences of the fabricated slot widths and variations of the sidewall roughness of the metallic slots.

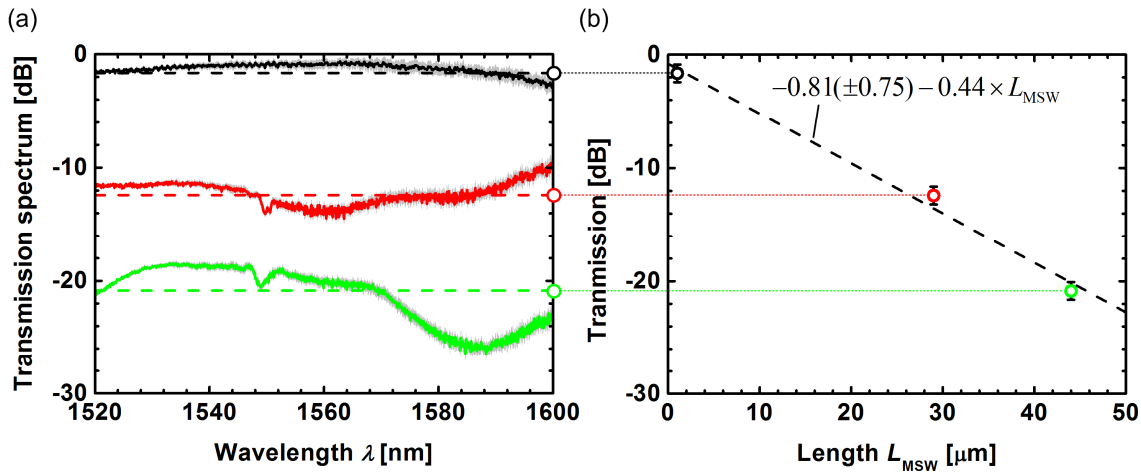


Figure 3- 9: Fabricated metallic tapered mode converters with three different MSW lengths L_{MSW} of (a) 1 mm, (b) 29 mm, and (c) 44 mm. The slot size h is about 140 nm for all three devices.

2.4. Static behaviour of plasmonic Mach-Zehnder modulators

Power transmission spectra for all three MZMs are given in Figure 3- 10(a). In addition, the transmission spectrum of a reference Mach-Zehnder interferometer is given without a plasmonic phase shifter. It can be seen that, that silicon grating couplers have a big contribution in the total insertion loss of our silicon-plasmonic Mach-Zehnder modulators. With the state of the art fiber to silicon-waveguide couplers with 1dB loss the total insertion loss of the current silicon-plasmonic Mach-Zehnder modulators can be reduced down to 13-20 dB depending on the length of the plasmonic phase shifters. The extinction ratio and the free spectral range (FSR) vary among the devices because of the uncertainty in defining the width and quality of the metallic slots. The shift of the wavelength corresponding to the minimum transmission with the applied voltage is measured in order to estimate the voltage U_p required for having a phase shift of p . An example of the transmission spectra for voltage off and on states are given in Figure 3- 10(b) for the MZM with the 39 μm long phase shifters. Measuring the wavelength shift Dl_0 for the applied voltage of U_0 , we calculating $U_p = Dl_{FSR} \times U_0 / (2Dl_0) \approx 30$ V for MZM with 39 μm long phase shifters and that the $U_p = 37$ V for the MZM with the 29 μm long phase shifter.. In particularly, we achieve on-chip electro-optic coefficient r_{33} in the range of 70 pm/V. This value is significantly lower than the maximum value of 110 pm/V specified for bulk. These values can further be improved by optimizing the poling procedure of the EO material and improving the fabrication of the metallic slots.

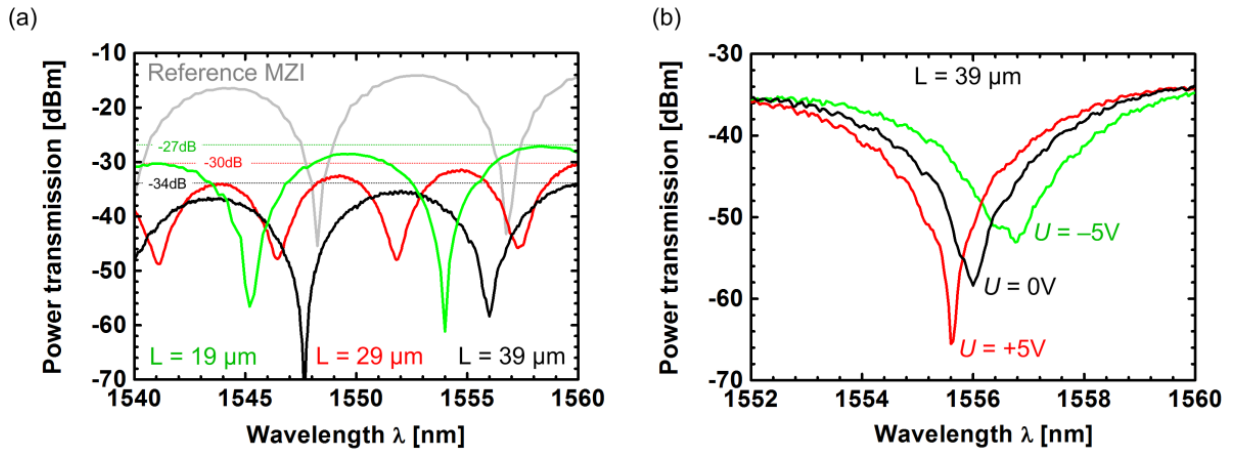


Figure 3- 10: Static characterization results for the Mach-Zehnder modulators. (a) Fiber-to-fiber power transmission is given for the MZMs with the length of 19 μm, 29 μm and 39 μm. In addition, we give the transmission spectrum of a reference Mach-Zehnder interferometer without a plasmonic phase shifters. The plasmonic phase shifters add 13 dB to 20 dB additional optical loss. (b) Transmission spectrum of the 39 μm long device is given for various applied voltages. Analyzing the shift of the wavelength corresponding to the minimum transmission we estimate the voltage U_p required for having a phase shift of π .

2.5. Data modulation

Next, data modulation experiments have been performed with the plasmonic MZM using a direct receiver setup as shown in Figure 3- 11(a). An electrical non-return-to-zero (NRZ) signal with PRBS pattern length of $2^{31}-1$ and with a peak-to-peak voltage swing of 5 V (measured across a 50 W resistor) is fed to the modulator via a ground-signal-ground (GSG) RF probe. The operating point for the MZM is defined by selecting the operating wavelength. The MZMs are operated in the quadrature points, i.e., the modulator output intensity changes linearly with the relative phase difference of the two arms. The OOK signal after the MZM is detected with a standard pre-amplified direct receiver comprising a single erbium doped fiber amplifier, an optical band-pass filter with a bandwidth of 2 nm, a bit-error-ratio tester (BERT), and a digital communication analyzer (DCA).

We measured the BERs for all three MZMs at a bit rate of 30 Gbit/s in order to find the optimum length for the phase modulators. During the experiment, the EDFA of the receiver is operated in constant output power mode. The input optical power to the modulator is varied from +10 dBm to +23 dBm. This varies the input power to the receiver, i.e., the optical signal-to-noise power ratio (OSNR) at the photodiodes. The optimum length of the PS is defined by a compromise between insertion loss and modulation index — making the device too short results in small optical modulation amplitude, while a too long phase modulator section decreases the receiver's input power. We find that in our case ($U_{pp} = 5$ V, SPP propagation losses of ~ 0.4 dB / μm , $r_{33} = 70$ pm/V) the optimum performance can be achieved with 29 μm long phase modulators, see Figure 3- 11(b). A better BER can be achieved by either increasing the optimum PM length L by improving the slot quality (decreasing optical losses), or by reducing the effective PM length by increasing the electro-optical coefficient and reducing the slot (increasing the optical modulation amplitude). The eye diagrams measured after the MZM with 29 μm long PM sections for bit rates of 30 Gbit/s ($\text{BER} = 2 \times 10^{-5}$), 35 Gbit/s ($\text{BER} = 3 \times 10^{-5}$) and 40 Gbit/s ($\text{BER} = 6 \times 10^{-4}$) are given in Figure 3- 11(c). These BER are well below the threshold of 4.5×10^{-3} for hard-decision FEC codes with 7% overhead. The driving voltages and the optical insertion losses can be further reduced by, first,

optimizing the poling procedure and thereby achieving higher electro-optic coefficients, second, reducing the slot size, and third, by using silver instead of gold.

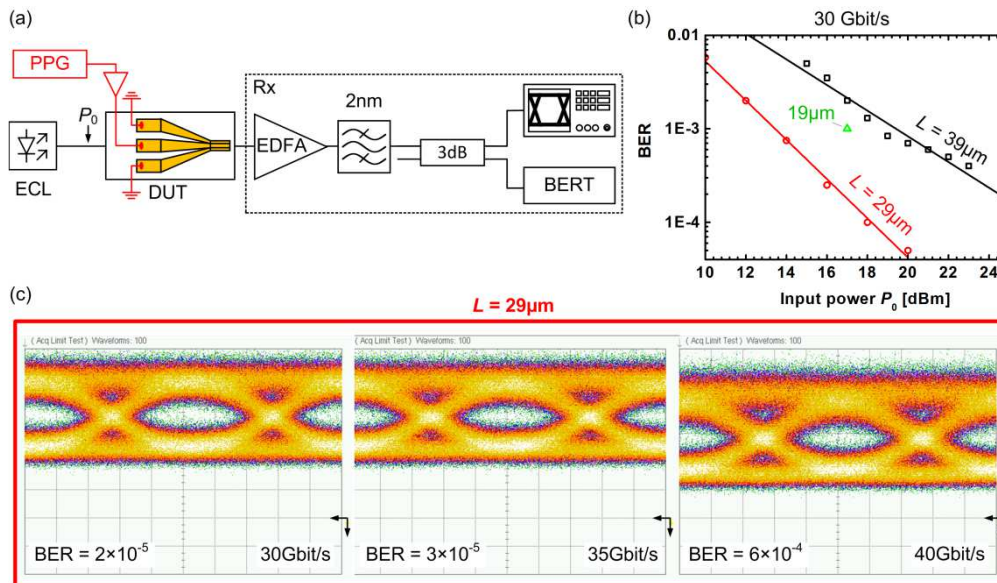


Figure 3- 11: Modulation experiments with plasmonic silicon-organic MZMs with PM lengths of 19 μm , 29 μm and 39 μm . (a) Direct receiver setup used for detecting on-off keyed signal after the plasmonic MZMs. (b) Bit error ratios measured for the MZMs with plasmonic phase modulator sections having lengths of 19 μm , 29 μm and 39 μm . To find the optimum phase shifter length, we vary the input power to the modulators and measure the BER. A compromise between the optical loss and the modulation index can be achieved by using a MZM with a PM length of 29 μm . (c) Eye diagrams measured at bit rates of 30 Gbit/s (BER = 2×10^{-5}), 35 Gbit/s (BER = 3×10^{-5}) and 40 Gbit/s (BER = 6×10^{-4}) for a MZM with 29 μm long PM sections at an input optical power of 20 dBm and at an operating wavelength of 1556.8 nm. The difference in the DC levels for data rates of 35 Gbit/s and 40 Gbit/s is attributed to the thermal drift of the operating point as a consequence of the large optical input power.

Deliverables in second intermediate reporting period (month 27 – month 36)

No deliverables were planned to be reported for the reporting period.

Milestones in second intermediate reporting period (month 27 – month 36)

No milestones were planned to be reached during the reporting period.

3.2.4 Work Package 4: Plasmonic Receiver

Task 4.1 Design and modeling of plasmonic pre-amplifier

a) Polymer based version

Task completed.

b) Hybrid silicon plasmonic amplifier

Task completed.

Task 4.2 Modelling of plasmonic QD polymer based photodetectors

Task completed.

Task 4.3 Colloidal quantum dots with optimized gain and electrical injection scheme

a) Characterization of HgTe-QD deposited as thin film

During the previous reporting period we demonstrated for the first time that HgTe QDs exhibited more interesting optical properties than those previously investigated on Pb-based quantum nanostructures, particularly longer exciton lifetimes and nearly thresholdless gain. All these measurements were carried out in solution though. To confirm that these results are also relevant towards development of integrated optical devices, during the current period we investigated the gain properties of HgTe QDs deposited in a thin film. Figure 4- 1) shows the absorption spectra of HgTe QDs before and after deposition (spin coated 3 times on Quartz). A slight red shifted is noted (50meV). These samples were then analysed using transient absorption spectroscopy. The analysis of the results learns us (Figure 4- 1b):

- There is still gain present, shifted to the red side
- The gain occurs at similar fluences as before
- The gain lifetime is reduced however to ~ 100 ps.

We believe that the gain lifetime could be increased again through optimising the deposition process and possibly the synthesis. The main issue relates to avoiding photocharging in film. This work is in progress. Measurements on thicker films prepared in vacuum conditions should be investigated, as should the newly synthesized HgTe QDOTs with narrower size dispersions.

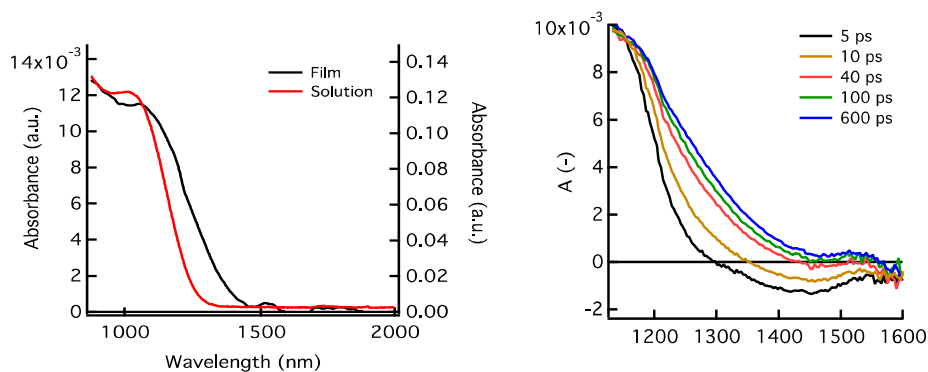


Figure 4- 1: (a) Absorption spectra for HgTe QDs in solution and in thin film and (b) non-linear absorbance A (note that gain corresponds to $A < 0$) for different delays under sub-1 exciton ($\langle N \rangle = 0.1$) conditions (note that standard QDOT threshold is 1).

b) Improved synthesis of HgTe QDs

Initial HgTe samples suffered from inhomogeneous broadening due to size dispersion, resulting in poorly defined absorption spectra (e.g. see Figure 4- 1a). During the current period the synthesis method was improved substantially, resulting in sharply defined absorption spectra (Figure 4- 2).

These samples have been measured also using transient absorption spectroscopy and we confirmed they still exhibit gain under similar conditions as before. As the synthesis method is quite different, this indicates the intrinsic nature of the thresholdless gain observed in HgTe QDOTS.

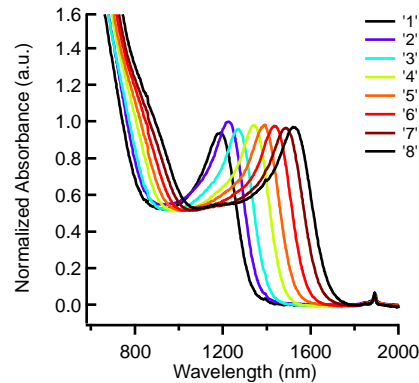


Figure 4- 2: Absorption spectra for HgTe QDs with improved synthesis (for different QD radius).

c) Electrical injection

New samples (ITO-SiN-QDOT-SiN-Au) have been prepared to test AC-electrical injection on QDOT structures. Hereby we used SiN (PECVD-deposited) barrier layers instead of AlOx (ALD-deposited) barrier layers because these are more compatible with the SiN waveguide platform under development. The operation of these devices was confirmed and the films seem to exhibit no pinholes, despite being deposited at low temperatures.

Task 4.4 Fabrication and characterization of QD-based plasmonic amplifiers

a) Polymer based version

During this reported period we have focus our work in developing plasmonic structures for a direct measure of the propagation length (L_p) of the surface plasmon polariton (SPP) modes and the effect of QDs-layers on L_p . Figure 4- 3 corresponds to different combinations of gold films and stripes (4 - 20 μm wide) 30 nm thick deposited on a SiO_2/Si substrate and cladded by a QD-PMMA (or bilayers QD-PMMA/PMMA) dielectric active waveguide. These waveguides allow the study of the SPP, but not all are able to propagate the pump beam by end-fire coupling, the most optimized optical pumping of QDs inside the polymer, as previously demonstrated in our studies. This is the case of the first design (Figure 4- 3a), the most simple to illustrate our method to determine L_p from the signal decay of the TM mode (associated to the LR-SPP), when increasing the distance between a probe fiber tip (where a laser at 533 nm is coupled to excite the photoluminescence at 600 nm of the CdSe QDs) and the sample edge (Figure 4- 4). The value deduced for $L_p \approx 12.5 \pm 2.0 \mu\text{m}$ is very close to the theoretical one at 600 nm, $L_p \approx 11 \mu\text{m}$. The TE mode exhibits smaller propagation losses (associated to absorption and scattering losses in the nanocomposite) with a characteristic decay around 60 μm .

The structure depicted in Figure 4- 3c would allow for an efficient pumping of QD emitters along the SPP propagation; it is based on a CdSe-PMMA/PMMA bilayer cladding the Au layer. Most of the emitted light is expected to couple to the LR-SPP, because this is the mode with the highest overlap with the nanocomposite. The TM signal exhibits higher propagation losses than that of TE and hence the first is associated to the propagation of the LR-SPP. The value of L_p is estimated in the range $10.4 \pm 2.1 \mu\text{m}$ (theoretical value = 11 μm), whereas increases up to 18.4 ± 1.7 and $25 \pm 8 \mu\text{m}$

under colinear pumping at 740 (red) and 2000 (green) W/cm^2 , respectively, as deduced from results in Figure 4- 5.

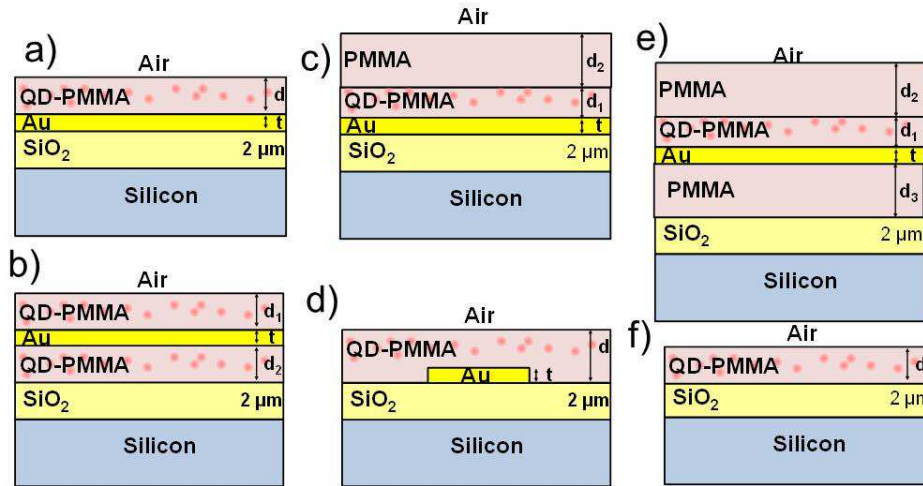


Figure 4- 3: Vertical cross-section of different plasmonic waveguides considered in this task.

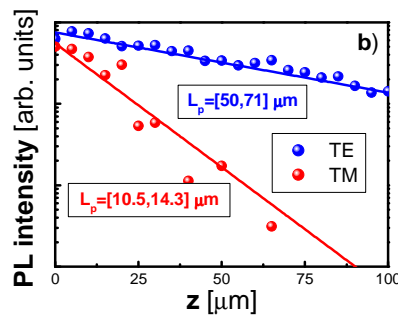


Figure 4- 4: Propagation length measured at 600 nm on a Au-film waveguide 30 nm thick cladded by a QD-PMMA nanocomposite ($ff=10^{-3}$, $d=1 \mu m$) on a SiO_2/Si substrate; the propagation length of the LR-SPP is obtained from the signal decay when increasing the distance between the tip and the sample edge.

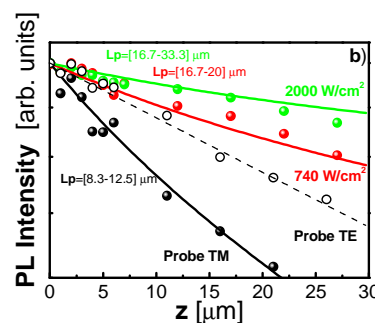


Figure 4- 5: Propagation length measured at 600 nm on a Au-film waveguide 30 nm thick cladded by a QD-PMMA/PMMA bilayer ($ff=10^{-3}$, $d_1=250 \text{ nm}$ and $d_2=2.5 \mu m$) on a SiO_2/Si substrate; the same conditions applies as in Figure 4- 4.

The structure depicted in Figure 4- 3d was our initial focus for this project, and preliminary results were shown in the last review report (using a gold stripe several micron wide) and some more

representative results are included in Deliverable 4.4. Our results yield a value of $L_p = 13 \pm 3 \mu\text{m}$ for the LR-SPP, which is enhanced when the pump beam is coupled in the dielectric waveguides up to $16 \pm 2 \mu\text{m}$ and $20 \pm 5 \mu\text{m}$ (for 740 and 2000 W/cm^2 of pumping power densities, respectively). More recently we have fabricated gold waveguides with some hundreds of nanometers of lateral side that will be used to finish this task by using improved HgTe QDs.

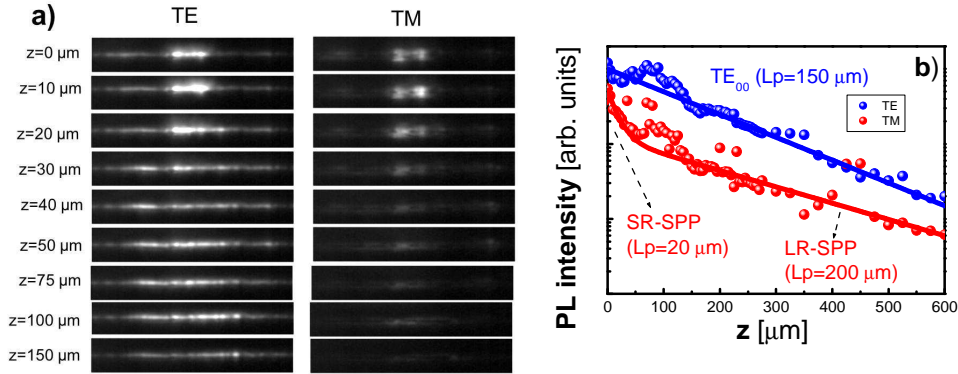


Figure 4- 6: Near field images (a) and detected signal as a function of the fiber tip to edge distance at $1.55 \mu\text{m}$ in the sample described in the text ($ff = 0.008$).

Finally, old HgTe QD material was used to corroborate the enhancement of L_p in plasmonic waveguides at infrared wavelengths, even if in this range we have the limitation of a worse signal-to-noise ratio (by the use of an InGaAs photodiode array instead of a Si CCD). Plasmonic waveguides were cladded by PMMA and the HgTe-PMMA nanocomposite by using the design shown in Figure 4- 3e (with only the bottom PMMA film to prevent metal roughness). Figure 4- 6 shows the fiber-tip characterization in a sample with $ff=0.008$, a concentration sufficiently low to consider that the structure is symmetric from the point of view of the dielectric constant, and hence the waveguide can support LR-SPP, SR-SPP and the TE_0 modes; higher order modes are not allowed for the thicknesses considered ($d_1 = 2 \mu\text{m}$, $d_2 = 0$ and $d_3 = 2 \mu\text{m}$). TM signal shows an intensity distribution centred at the metal and suffers a higher attenuation, as compared to TE (Figure 4- 6a). On the other hand, TM signal exhibits two decays (red data in Figure 4- 6b), the faster one ($L_p \approx 20 \mu\text{m}$) attributed to the SR-SPP mode and the slow one ($L_p \approx 200 \mu\text{m}$) to the LR-SPP. These experimental values are not far from the ones obtained in the simulations: 11.4 and $900 \mu\text{m}$ for the SR-SPP and LR-SPP modes, respectively. The shorter experimental value of L_p for the LR-SPP as compared to the simulations is associated to roughness in the nanocomposite. For this waveguide any L_p enhancement of the SPP modes was observed after the end-fire coupling of a laser beam for QD pumping, possibly due to the low ff used. In this way a second sample was fabricated with a similar structure, but $ff = 0.08$; however, the symmetry of the refractive index above/below the gold layer is now broken and the LR-SPP cannot longer exist. The TM signal has a clearly different intensity distribution and a larger attenuation as compared to that of TE (Figure 4- 7a). The dependence of the guided TM-light as a function of the distance tip-edge also exhibits a double exponential decay (black data in Figure 4- 7b), characterized by $L_p(1) \approx 18 \mu\text{m}$, associated to the SR-SPP, and $L_p(2) \approx 67 \mu\text{m}$ that we attribute to an hybrid photonic-plasmonic mode (see D4.4). After coupling a pump beam to the input edge of the sample L_p of both modes is enhanced by a 15% (red curve of Figure 4- 7b), approximately.

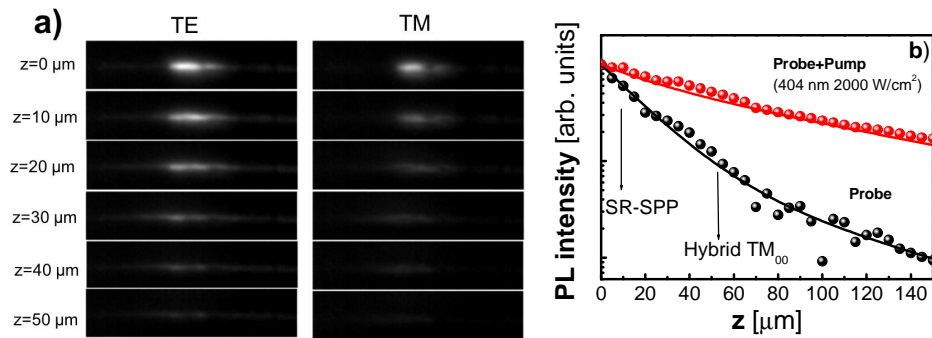


Figure 4- 7: Near field images (a) and detected signal as a function of the fiber tip to edge distance at 1.55 μm without (black) / with (red) optical pumping of QDs (b) in the sample described in the text ($f\beta = 0.08$).

b) Hybrid silicon version

To characterize the gain of our QDs we prepared a SiN-waveguide platform allowing us to carry out a variable stripe based measurement to extract the gain. Figure 4- 8a shows SiN partly covered with CdSe QDs (increasing length from top to bottom). Figure 4- 8b shows the measurements for one set of waveguides, under CW pumping. In case of gain this curve should show a superlinear trend, which is not the case here. We are currently preparing a setup to pump these devices under pulsed conditions with high peak power.

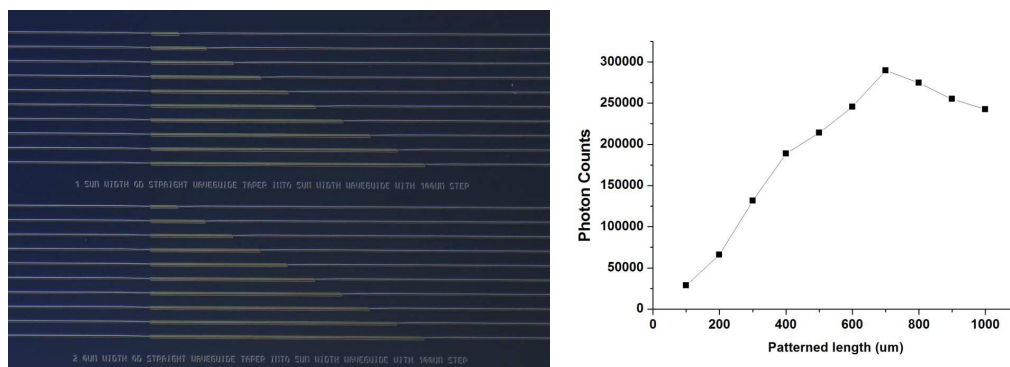


Figure 4- 8: a) Microscope view of SiN with variable length QD-pattern on top. b) Power emitted at 600 nm as function of length.

c) Preparation of DBR-mirrors for realization of liquid cavity

We prepared DBR-mirrors (a-Si/SiOx) to realize a VCSEL-like cavity with the HgTe QDOTs as the gain material. This will allow us to demonstrate even more convincingly that the QD medium does show gain.

Task 4.5 Fabrication of plasmonic polymer QD based photodetectors

a) Schottky-heterostructure photodiodes

In the last months we have optimized the synthesis of PbS QDs with absorption/emission at wavelengths around 1550 nm (Figure 4- 9a), as also the deposition (+ ligand exchange) of thin films in the thickness range 300-500 nm by means of a Dr.Blading technique. These layers exhibit a

reasonable uniformity throughout the sample, as revealed by exciton absorption and photoluminescence (PL) spectra very close to those in colloidal solution (Figure 4- 9a-b); a complete ligand exchange is produced after several minutes, which is translated in a smaller PL signal (higher conductivity by electronic coupling between QDs). Layers with completed ligand exchange have a resistivity around $10^5 \Omega\text{cm}$, a hole concentration larger than 10^{15}cm^{-3} and mobilities smaller than $0.065 \text{cm}^2/\text{Vs}$, as estimated from preliminary Hall measurements.

The Dr.Blading technique substantially decreases the effect of granularity/roughness obtained in first device generations based on spin-coating that was limiting, presumably, the I(V) and responsivity of photoconductors/photodetectors prepared by this method. We have continued producing PbS QD films on glass (for micro-gap photoconductors) and glass/ITO/PEDOT (for Schottky/heterostructure photovoltaic photodetectors) substrates, finishing the devices by using Ag electrodes. In the two most recent device generations after the last review report we have consolidated responsivities above 0.1 A/W under continuous wave illumination at 1550 nm (0.16 A/W at the exciton peak wavelength, 1620 nm), as shown in Figure 4- 9.

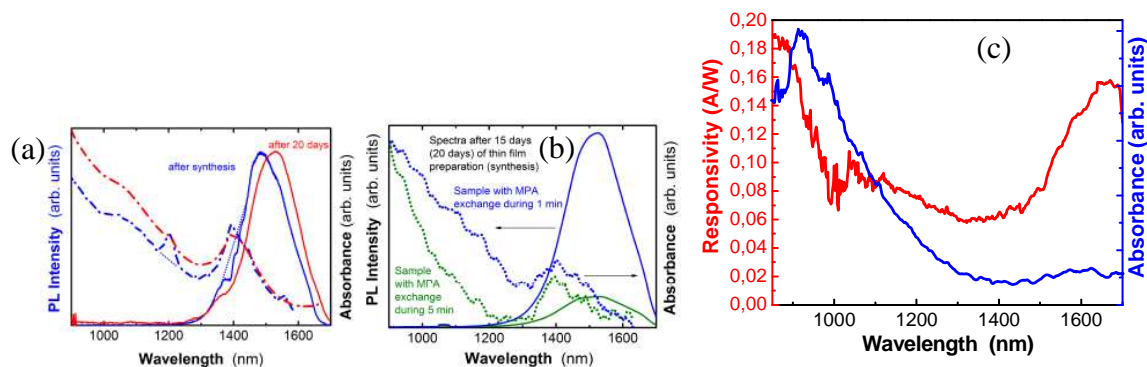


Figure 4- 9: Absorption and photoluminescence spectra of a PbS QD colloid (after synthesis and 20 days later) (a) and QD-layers 500 nm thick prepared by Dr.Blading and ligand exchange during 1 (uncompleted) and 5 (completed) minutes (b); (c) Responsivity (red) and absorbance (blue) curves of one of the best Schottky photodiodes measured during the first days after fabrication.

We have also measured these Schottky diodes under laser illumination at 1550 nm as a function of power (Figure 4- 10). The I(V) characteristics exhibits can be fitted by using a real equivalent circuit for the photodiode that yields a dark current around 70 nA with an ideality factor around 3 (carrier generation-recombination mechanism) and shunt resistance (attributed to hole losses through the Ag electrode) decreasing with increasing illumination. The lowest detected power was 6 nW by using our Keithley 2400 source-meter, hence the noise equivalent power is smaller than this value (under continuous wave excitation). The photocurrent is practically linear (exponent = 0.92) with power from 6 nW ($I_{cc} = 0.8 \text{ nA}$, $V_{oc} = 9 \text{ mV}$) to $2 \mu\text{W}$ ($I_{cc} = 190 \text{ nA}$, $V_{oc} = 70 \text{ mV}$) and $R \approx 0.1 \text{ A/W}$ in the entire range. The newest generation of photodiodes (under characterization) will serve us to measure other important parameters and figures of merit for Schottky-heterostructure photodiodes and characterization as a function of temperature, prior to introduce a stopping layer for holes (to increase fill factor, reduce noise current and increase of V_{oc}) and plasmonic effects (to increase light trapping and near-field absorption at the QD layer).

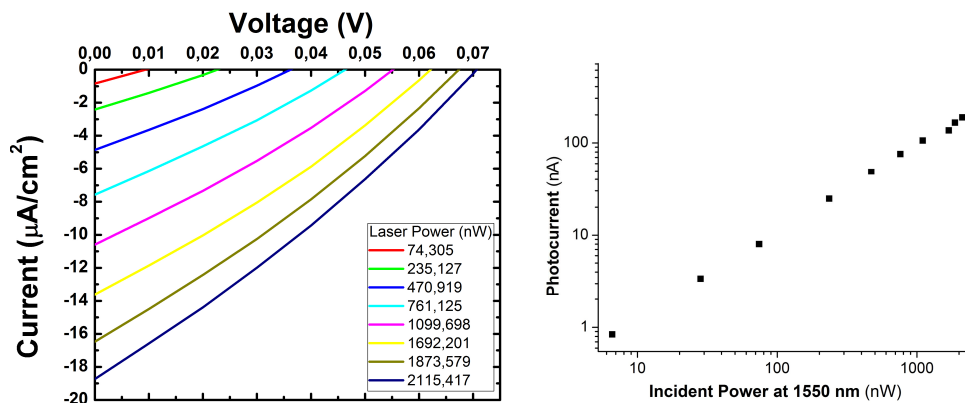


Figure 4- 10: (a) I(V) characteristics of the best ITO/PDOT/PbS-QD-solid/Ag photodiode (at 1550 nm) under illumination with a laser at 1550 nm at different powers; (b) power dependence of the measured photocurrent.

b) QD-solid based microgap/nanogap photoconductors

The Schottky concept is a very convenient device to be integrated in SOI technology, because photocurrent or photovoltage can be directly measured without needing of polarization or used as input for a transimpedance amplifier. Given that most of the work on Schottky diodes is already finished our goal is to concentrate our effort on photoconductive devices. In the case of nanogap, given the small distance between electrodes and high electric field we do not plan to use ligand exchange on deposited QDs. In the case of microgap we have develop a first generation of interdigitated electrodes (Figure 4- 11), for which appreciable photocurrent is measured at 1550 nm in preliminary tests, even if we are not satisfied with the ligand exchange protocol on small area QD-layers. In this sense, in a photoconductive device (0.2 mm gap) made these days on a QD-layer prepared as in the Schottky device (complete ligand exchange) we arrive to photocurrents ≈ 30 -50 nA (responsivities very close to 0.1 A/W) in the wavelength range 1200-1500 nm at 200 V bias (see Table 4- 1), despite the big distance between electrodes, over a reasonably low dark current (49 nA).

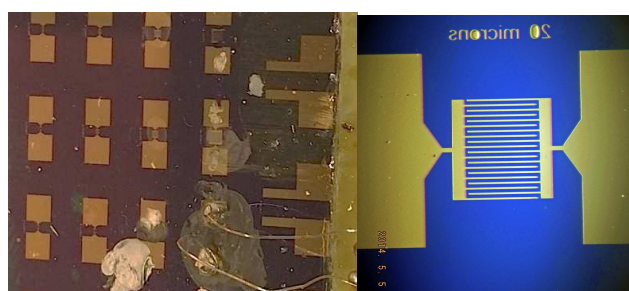


Figure 4- 11: Photograph of interdigitated photoconductors with a QD-layer on one of them and zoom image of one of them (20 μm gap).

λ_i (nm)	P_i (μ W)	I_{ph} (50 V)	I_{ph} (200 V)	R (50 V) mA/W	R (200 V) mA/W
650	45	98	528	2.2	11.7
1200	0.53	10.5	50	19.8	94.3
1300	0.25	6.1	29	24.4	116
1400	0.4	6.8	32	17	80
1500	0.46	8.4	34	18.3	74
		$I_{dark} = 11$ nA	$I_{dark} = 49$ nA		

Table 4- 1: Measured values of photocurrent (over dark current values indicated at the bottom) and responsivities at different wavelengths for 50 and 200 V bias.

As next steps we will try to improve microgap photoconductor devices by means of developing a good protocol for ligand exchange in the QD-film and concentrate on plasmonic nanogap photoconductors.

Status deliverables and milestones

MS24	Demonstration of SPP amplifiers with electrical injection exhibiting 10dB/cm gain	4	UVEG	30	01/2014
------	---	---	------	----	---------

MS24 is pending. Necessary to ask for a delay.

D4.4	Report on SPP amplifiers by using QDs	4	IMEC	30	4/2014
D4.5	Report on plasmonic photodetectors	4	UVEG	42	9/2014

D4.4 is finished without using optimized HgTe material. Target results would be expected with optimized material along next months.

Use of resources (months 24-36)

The table below gives a review of each partner contribution.

Partner	Person power	Main contribution
UVEG		Fabrication and characterization of QD based photonic/plasmonic structures for amplification, study of quantum dot based photodetectors (Schottky, micro/nanogap).
UGent		Synthesis of colloidal nanoparticles, its fundamental optical properties in colloidal state and layers.
IMEC		Fabrication and characterization of silicon hybrid plasmonic amplifiers. Electrical injection devices.

3.2.5 Work Package 5: Optical and Electrical Interfaces

Task 5.1 Modelling and fabrication of coupling Si waveguide to plasmonic waveguide

Task completed during previous period

Task 5.2 Design and fabrication of Si beam shaper

In the previous period we investigated the design and applicability of focusing grating couplers. One of the main conclusions was that due to fundamental limitations related to the diffraction of light such grating couplers can not substantially increase the connection capacity between two chips (which is equal to number of links x single link capacity). Nevertheless, we prepared designs of such focusing grating couplers to be fabricated. In the current period the fabrication of these designs was started. We will thereby make use of the standard silicon platform described earlier to make the base structures and on which we will afterwards defined low index contrast grating patterns using ebeam lithography (the standard silicon platform does not allow for sufficient low index contrast etching to define the desired focusing gratings. Fabrication of the base circuits has started.

Task 5.3 Design and fabrication of passive ultra-compact components as filters

Task completed during previous period

Task 5.4 Signal generation module design

The **Dual Die Communication Module** (abbreviated **DDCM**) is the building-block responsible for the interconnection of different dice within a so called Network in Package (NiP), the communication system enabling inter dice data transmission in the context of Systems in Package (SiP) technology.

According to a widely used approach, the DDCM is seen composed of two main building blocks:

- the DDCM **controller**, responsible for managing incoming/outgoing STNoC/SBus/AMBA-AXI traffic, generating IDN segments through encapsulation and preparing them to be sent to the PHY transmitter, as well as collecting them from the PHY receiver;
- the DDCM **PHY**, responsible for transmitting output phyts across the physical link and collecting inputs phyts from the physical link.

As shown in Figure 5- 1, the DDCM top level in each die consists of a transmitter (DDCM Tx) and a receiver (DDCM Rx).

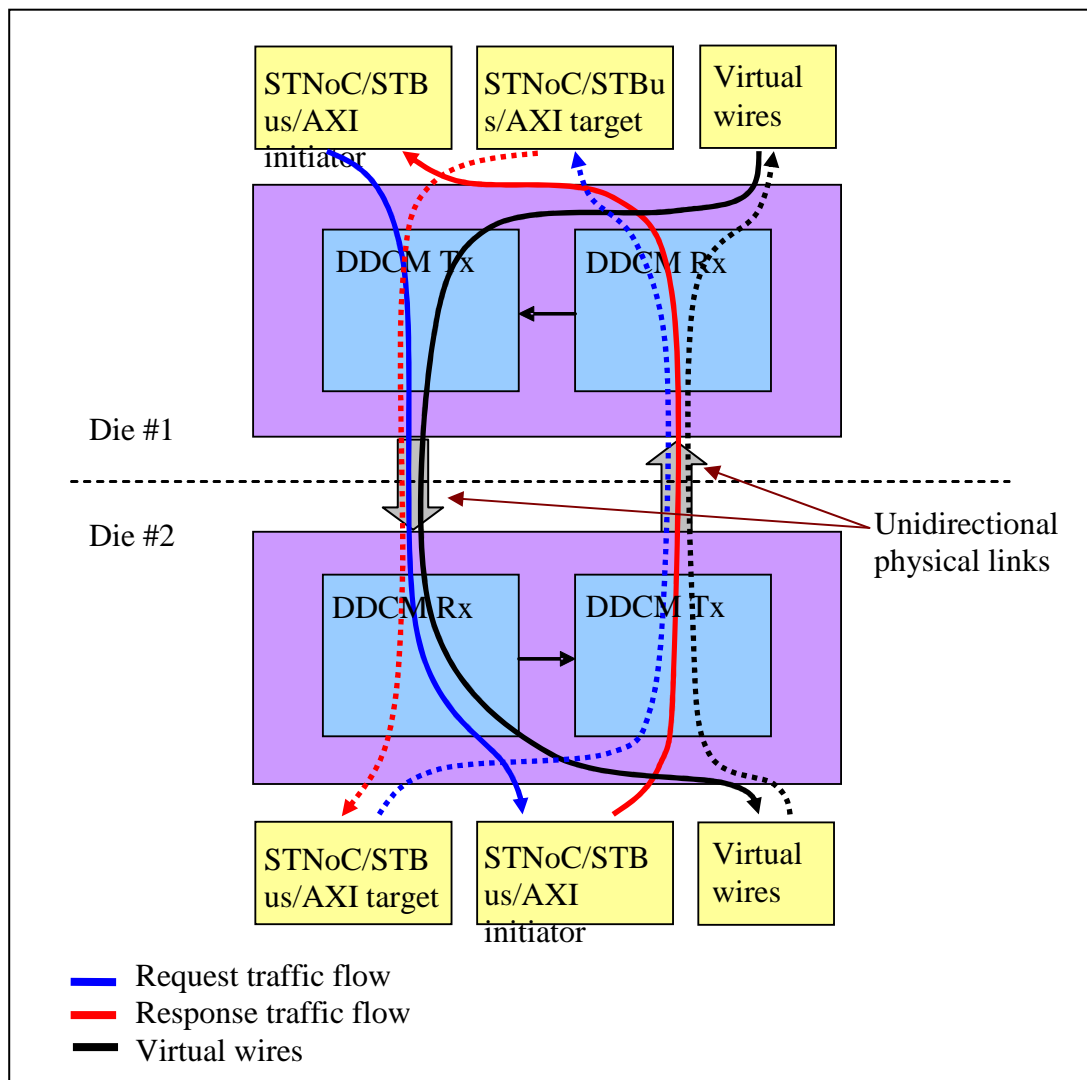


Figure 5- 1: DDCM top level architecture and information flow

In such a figure it's possible to see the two information flows supported by a complete DDCM architecture, i.e.

- requests from STNoC/STBus/AMBA-AXI initiators in chip 1 to STNoC/STBus/AMBA-AXI targets in chip 2, responses from STNoC/STBus/AMBA-AXI targets in chip 2 to STNoC/STBus/AMBA-AXI initiators in chip 1, virtual wires from chip 1 to chip 2 (continuous lines);
- requests from STNoC/STBus/AMBA-AXI initiators in chip 2 to STNoC/STBus/AMBA-AXI targets in chip 1, responses from STNoC/STBus/AMBA-AXI targets in chip 1 to STNoC/STBus/AMBA-AXI initiators in chip 2, virtual wires from chip 2 to chip 1 (dotted lines).

The DDCM is a **parametric** design that, depending on the SoC where it is used, can be configured properly in order to meet system requirements and needs in terms of interfaces, FIFOs sizes, clock domains synchronization and functionality.

So as for the DDCM with electrical PHY, a VHDL model of the plasmonics-based PHY has been developed in order to be co-simulated with the digital parts of the DDCM described as synthesizable VHDL

The DDCM data base is located in the ST Interconnect System Group server design area under the directory **ddcm_lib** identifying the design library.

The **ddcm_lib** directory contains the following two subdirectories:

- **dev** (development) containing the generic design and the generic verification environment;
- **run** containing the simulation area for a set of specific configurations of the design.

The directory **dev** contains the following subdirectories:

- **doc** containing the functional specification of the block (deliverable D5.4 in NAVOLCHI project context);
- **rtl_vhdl** containing the VHDL files representing the rtl description of the DDCM top level and all its building-blocks;
- **model** containing the VHDL files representing the rtl behavioural description of the analog building-blocks and the plasmonic devices implementing the plasmonics-based PHY;
- **corekit** containing the generic view of the DDCM;
- **verif_env** containing the generic verification environment, i.e. testbench and stimuli sources;
- **verif_run** containing the tests to verify the different functionality of the DDCM;
- **synth** containing the area for the logic synthesis of the DDCM.

The design environment consists of the directory **rtl_vhdl** and **corekit**.

In the **rtl_vhdl** directory there are the files describing VHDL entity and architecture of the DDCM top level and all its building-blocks (i.e. transmitter, receiver, FIFOs, etc.)

All these blocks are described following a parametric approach, so that after setting a proper set of parameters to the required values, the generic design gets configured accordingly and becomes specific for a well defined application. As described in the DDCM functional specification (deliverable D5.4) the design parameters allow to characterize the DDCM in terms of interfaces size, FIFO depth, traffic management policy, clock frequencies, etc.).

The VHDL description is *technology independent*, that is to say the VHDL files describe the structure and the functionality of the DDCM, with no links with the CMOS technology with which the DDCM itself will be implemented.

In the **model** directory there are the files describing the VHDL behavioural models of the analog electronic parts (modulator driver, TIA, comparator) and the plasmonic devices (emitter, modulator, waveguide, detector) to be co-simulated with the digital parts of the DDCM.

The **corekit** directory contains a set of scripts allowing to build the so called *corekit*, a file containing all the information about the generic design and allowing by means of a GUI (Graphic User Interface) the user to assign the required values to the design parameters and getting a specific configuration of the DDCM, moving from the generic description.

The verification environment, strongly based on the one developed for the DDCM with electrical PHY, consists of the directories **verif_env** and **verif_run**.

The **verif_env** directory in turn contains the following main subdirectories:

- **rtl_tb** containing the VHDL testbench, i.e. the structure instantiating the DDCM and the plasmonics-based PHY behavioural model, considered the **DUT** (Device Under Test) and the traffic generators for stimulating the design and verify its behaviour accordingly;
- **e** containing the functional description of the traffic generators in *e* language, an object oriented high level language specific for verification suites;

- **config_files** containing a variety of files with different set of design parameters so to configure the DDCM in different ways in order to verify as many different specific implementations as possible;
- **tests** containing the description of different tests, aiming at stimulating the different DDCM functionalities.

The `verif_env` directory contains generic descriptions of all the structures described in it (testbench, stimuli generators, tests); the `verif_run` directory contains a replication of the `verif_env` subdirectories but configured according to the design parameters, and the specific for a well defined application or product employing the DDCM.

Task 5.5 Signal Generation Module implementation via FPGA

After digital design and functional verification phases, the developed rtl code has been synthesized in order to get a gate level netlist, representing the Front-End view (schematic) of the DDCM.

The synthesis environment consists of the directory **synth**.

This in turn contains the following subdirectories:

- **input** containing the configured VHDL code for a specific DDCM implementation;
- **scripts** containing the commands for the synthesis tool;
- **run**, the directory where the synthesis tool is invoked and log files are recorded;
- **reports** containing the characterization of the synthesized design in terms of area, timing (speed) and power consumption
- **output** containing the synthesized DDCM design in terms of Front-End netlist.

The generic DDCM synthesis environment is fully based on **Synopsys** tools, i.e. **Design Compiler** as synthesis engine and **Design Vision** as interactive GUI.

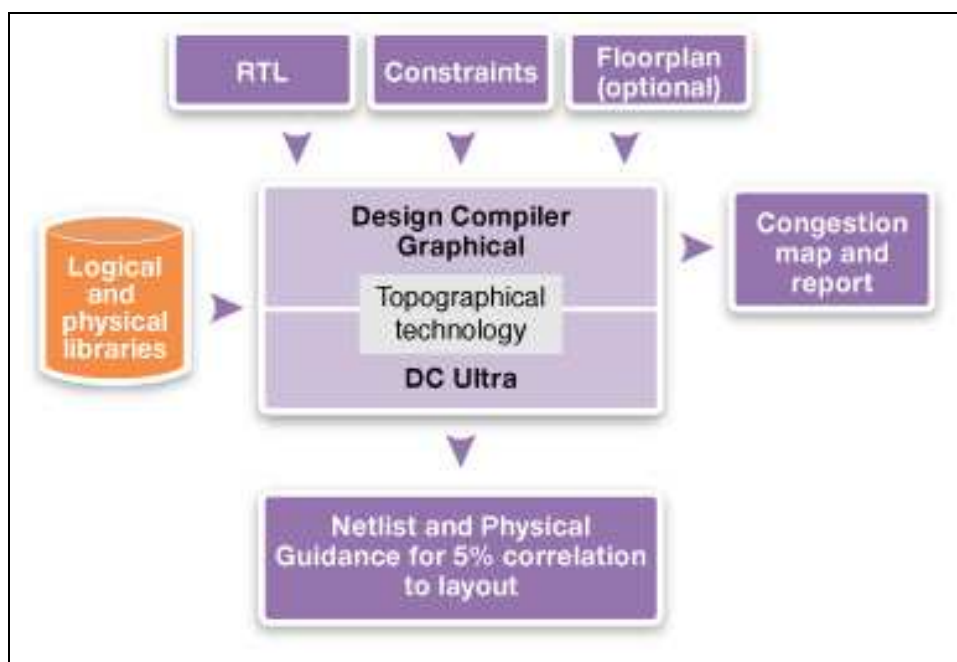


Figure 5- 2: Synthesis flow based on Synopsys Design Compiler

The synthesis design phase is strongly technology dependent, since the results of the synthesis process, i.e. the gate level netlist, is an assembly of technological standard cells implementing the structure and the functionality of the DDCM in the required technology.

Also the version the DDCM supporting a plasmonics-based PHY has been synthesized using 65nm and 40nm CMOS technologies. Of course no synthesis activities have been carried out for the analog parts and for the plasmonic devices composing the plasmonics-based PHY, since a specific full custom design is required for them.

Based on the Synthesis environment, a flow for the characterization of the digital parts of the DDCM in terms of power consumption has been developed, as shown in Figure 5- 3.

According to this flow a specific configuration of the DDCM is simulated many times, and for each simulation the switching activity at each node and across each wire of the design is recorded; then this switching activity is back-annotated on the netlist in Design Compiler environment, and the power analysis tool is invoked so to calculate the power consumed by the DDCM block taking into account the switching activity determined by the traffic injected in different scenarios.

Relying on the obtained data, average and peak power consumption is determined. However the contribution of the digital parts to the power consumption of the overall system is negligible, since the highest contribution is expected to come from the plasmonic components.

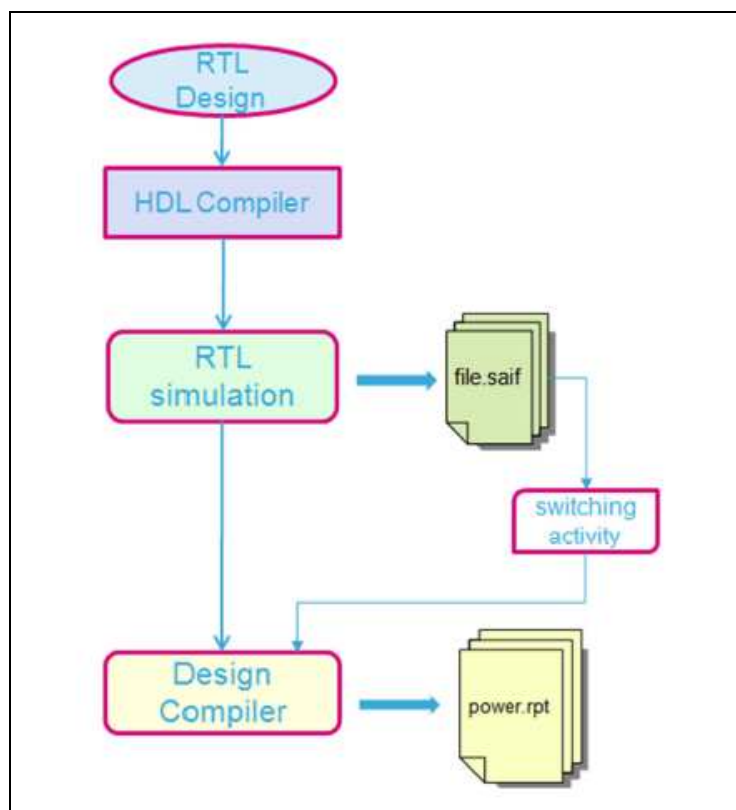


Figure 5- 3: Power consumption characterization flow

After synthesis and characterization flows have been carried out, the DDCM rtl code has been synthesized for FPGA mapping, exploiting ZeBu equipment and realted environment. The synthesis flow for FPGA is fundamentally the same as the one already described; the main difference is in the synthesis engine, that instead of translating the rtl design into a set of standard cells exploiting technology libraries, translates the rtl design into a set of logic structures that can be mapped into the hardware basic logic structures available in the ZeBu FPGA chip. The mapped FPGA has then

been stimulated and functionally validated with a verification environment very similar to the one used for rtl functional verification, the main difference being in the DUT; not an rtl code anymore, but an FPGA chip connected to the PC via a parallel interface, across which stimuli go from verification environment to FPGA, and FPGA reactions go back to verification environment.

Studies on DDCM architecture evolution for making it suitable to be used in more complex multi-dice systems implementing a so called Network in Package (NiP) have not been carried out since after a recent company reorganization, ST divisions have no longer interest towards this kind of solutions for consumer products.

Status deliverables and milestones

WP5 Completed Deliverables

D5.1	DDCM specification document	5	ST	6
D5.2	DDCM with electrical PHY design and verification data base	5	ST	12
D5.3	Compact optical filters (2nm bandwidth, >30nm FSR) and first generation beam shapers	5	IMEC	21
D5.4	Generic DDCM compatible with plasmonic-based PHY specification document	5	ST	24
D5.5	Report on plasmonic waveguide couplers	5	KIT	24
D5.6	Generic DDCM compatible with plasmonic-based PHY design and verification data base	5	ST	39

WP5 Deliverables for coming period

D5.7	Second generation beam shapers (distance 1mm, with bandwidth > 10nm and efficiency > 3dB)	5	IMEC	42
------	---	---	------	----

WP5 Completed Milestones

MS25	Decision on optimized plasmonic waveguide couplers	5	KIT	6	04/2012
MS26	Fabrication of plasmonic waveguide couplers with less than 3 dB coupling loss	5	KIT	12	10/2012
MS27	Design of first generation beam shapers and compact optical filters	5	IMEC	12	10/2012
MS28	DDCM with electrical PHY design and verification	5	ST	12	10/2012
MS29	Data codecs for power consumption reduction	5	ST	15	01/2013
MS30	Decision on plasmonic waveguide couplers with less than 3 dB coupling loss	5	KIT	15	01/2013
MS31	Fabrication of compact optical filters and first generation beam shapers	5	IMEC	18	04/2013
MS32	Data codecs for error detection and correction	5	ST	18	04/2013
MS33	Design of second generation beam shapers	5	IMEC	24	10/2013
MS34	Generic DDCM compatible with plasmonic-based PHY	5	ST	24	10/2013

WP5 Upcoming Milestones

MS35	Fabrication of compact optical filters and first generation beam shapers	5	IMEC	39	01/2015
MS36	DDCM evolution for NiP solutions	5	ST	39	01/2015

Use of resources (months 24-36)

The table below gives a review of each partner contribution.

Partner	Person power	Main contribution
IMEC	2	Fabrication of focusing grating couplers
KIT	0	Activity completed
ST	9	DDCM design and verification activities completed Study of DDCM evolution for NiP application not carried out because of ST interest change

3.2.6 Work Package 6: Integration, Characterising and Testing

Deliverables

Deliverables in third reporting period (M27-M36)

D6.1: Report on characterization results of all plasmonic devices [M27]
This deliverable was submitted in M36.

D6.2: Report on characterization results of all optical interface plasmonic passive components [M27]
This deliverable was submitted in M36.

Upcoming Deliverables

D6.3: Report on chip to chip interconnect characterization [M45]

D6.4: Report on plasmonic system-in-package interconnect prototype testing and evaluation [M45]

Milestones

Milestones in third reporting period (M27-M36)

MS39 Concept for system integration developed [M27]

This milestone is largely completed but under continuous update to incorporate the latest developments and results from ETH.

Upcoming Milestones

MS40 Individual plasmonic devices characterization, testing and evaluation [M39]

MS41 Chip to chip interconnect characterization [M42]

MS42 Plasmonic components integration to demonstrate chip-to-chip interconnect [M42]

MS43 Plasmonic chip to chip interconnect prototype testing and evaluation [M45]

Task 6.1: Characterization of active and passive plasmonic devices

The aim of this task is the characterization of individual plasmonic devices. The devices comprise a nanolaser, a modulator, an amplifier and a detector, from which the last three are based on plasmonic effects.

Nanolaser: Concerning the nanolaser, the core technology required for the fabrication has been developed. Different lithography schemes were proposed and successfully demonstrated for the accurate definition of the nano-cavity, and sub-micron waveguide and grating coupler structures. Silver-based ohmic contacts were fabricated and characterized for membrane photonic circuits which showed a contact resistance as low as $0.5 \cdot 10^{-8} \Omega\text{cm}^2$. This fabrication technology is used in the latest fabrication run that aims to demonstrate operating laser devices.

Modulator: High speed plasmonic-organic hybrid (POH) Mach-Zehnder modulators are demonstrated operating at the data rates of up to 40 Gbit/s. We report on on-off keying (OOK) signaling with POH Mach-Zehnder modulators (MZM) at data rates of up to 40 Gbit/s with low energy consumptions of 75 ... 225 fJ / bit. In particular, using the 29 μm device we show OOK signaling at data rates of 30 Gbit/s, 35 Gbit/s and 40 Gbit/s with the BERs well below the hard-decision FEC threshold. The measured BERs represent the lowest values, and therefore clearly demonstrating the applicability of plasmonic devices particularly in short-reach optical links.

In addition, we demonstrated a latching optical switch that combines the memristor concept with plasmonics. The switch exploits the formation and elimination of a conductive path in the insulating layer of a metal – insulator – metal layer stack. The conductive path leads to an attenuation of the optical mode in the OFF state and is ruptured when switching to the ON state. The plasmonic switch is integrated with a silicon photonic waveguide. Optical extinction ratios of 12 dB at 1550 nm wavelength are shown for 10 μm long devices. The operation power is consumed only when the state of the switch is changed and is below 200 nW with operating voltages in the range of 2V and currents below 100 nA. Tests with 50 write cycles and sinusoidal modulation in the megahertz regime demonstrate excellent repeatability of the switching mechanism.

Amplifier: Two concepts of hybrid-plasmonic amplifiers incorporating QDs (using polymer and SiN waveguides) have been fabricated and characterized by using CdSe QDs emitting at visible and HgTe QDs emitting at NIR wavelengths. Metal waveguides (planar and ridges) have been fabricated and used to investigate the observed increase of the SPP propagation length by optical pumping of QDs, even if net gain cannot be achieved by the available material.

Photodetector: In the case of photodetectors based on quantum dots important advances have been reached during the last year: i) reproducible and optimized conductive films of PbS QDs prepared by Dr. Blasing were achieved along several series of devices, ii) the best value for the responsivity in Schottky-heterostructure photodetector was around 0.16 A/W at the exciton peak absorption (≈ 1620 nm), iii) the best value of dark current was 70 nA with an ideality factor around 3, using Ag electrodes, iv) at 1550 nm, where $R \approx 0.1$ A/W, pumping light above 6 nW can be detected. Plasmonic photoconductors by considering a plasmonic nano-gap waveguide concept were fabricated (in collaboration with TUE-group) and are under characterization.

Task 6.2: Assembly and packaging of plasmonic devices into System in Package

This task led by KIT aimed at the assembly and packaging of receiver and transmitter. In particular, the optical link between the two parts were investigated.

As decided by the consortium, the system demonstration follows the contingency plan as depicted in Figure 6- 1.

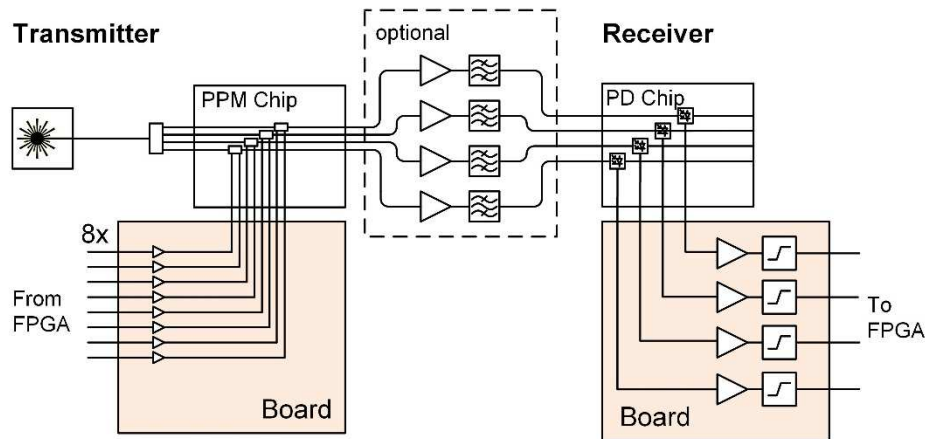


Figure 6- 1: Contingency Plan

On the transmitter side, the plasmonic phase modulators (PPM) that were successfully demonstrated in Task 6.1 are used. Light from an external laser source are split into four optical channels either off- or on-chip, before it is fed to the plasmonic modulator chip. The electrical signal is provide by an FPGA and amplified on an electronic board. The modulator chip is connected to the latter by electrical wire bonds.

On the receiver side, commercial photodetecor (PD) arrays fabricated by IMEC are used. The electrical signal is fed to transimpedance limiting amplifiers on an electronic board, before being sent to the FPGA.

For the optical link between transmitter and receiver, two packaging scenarios were compared (see Figure 6- 2): The 2D in-plane packaging with fiber interconnects and the 3D vertical stacking using a free space communication channel. As described in deliverable 6.2, the 2D in-plane packaging was found to be the most promising scenario. State-of-the-art fiber arrays (from Chiral Photonics, Inc.) shall provide four optical channels with a pitch size of 50 μm . Note that very low cross talk was demonstrated even in the case of 20 μm channel pitch sizes [1]. Moreover, this packaging scenario provides enough space for electrical wires between the PCB board and the silicon photonic chips. Optical amplifiers between transmitter and receiver can easily be integrated, if necessary. The challenge of this approach is the high alignment accuracy required when aligning the fiber array to the silicon photonic chips.

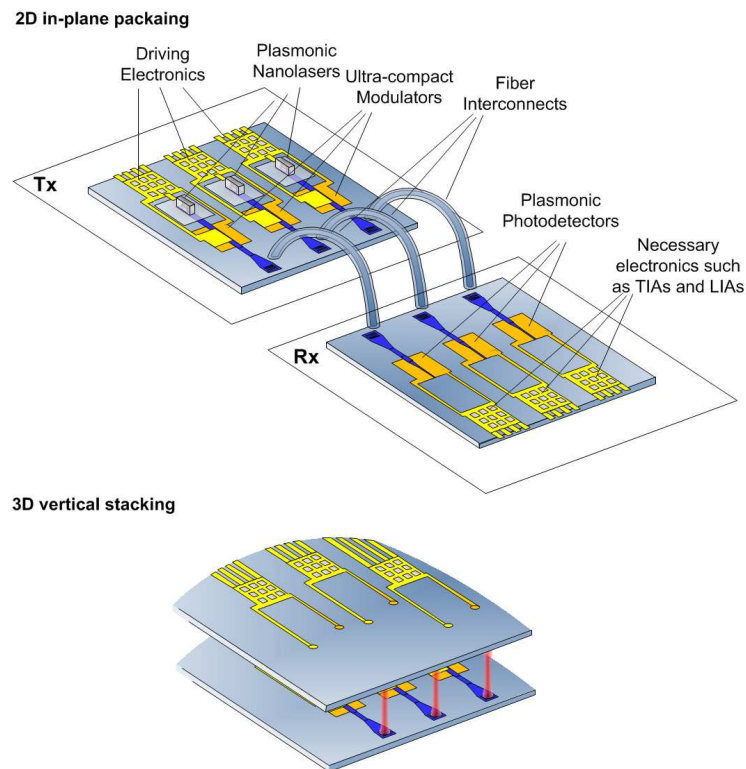


Figure 6- 2: Two packaging architectures considered in NAVOLCHI

1. F. E. Doany, B. G. Lee, S. Assefa, W. M. J. Green, M. Yang, C. L. Schow, C. V. Jahnes, S. Zhang, J. Singer, V. I. Kopp, J. A. Kash, and Y. A. Vlasov, J. Lightwave Technol. **29**, 475 (2011).

3.2.7 Work Package 7: Exploitation and Dissemination

General Status

During the last period of NAVOLCHI all tasks (Task 7.1 (Dissemination) and Task 7.2 (Exploitation) and Task 7.3 (Promotion)) have been active. NAVOLCHI partners have contributed several publications to high-quality scientific journals, magazines and conferences disseminating project results. Communication has been established with another plasmonics-related EU-funded project (PLATON). The NAVOLCHI consortium is committed to the continuation of the dissemination and exploitation effort.

Task 7.1 Dissemination

Dissemination of ideas and results is of high importance in the NAVOLCHI project. The partners of NAVOLCHI are top research organizations with proven track records in their field and are very active in disseminating research results in a worldwide range to scientists, industry, and the public.

Dissemination activities this far

There has been significant dissemination action concerning NAVOLCHI activities and results as it is shown in the following list:

AIT :

- 'Plasmonic Communications: Light on a Wire' Leuthold, J.; Hoessbacher, C.; Muehlbrandt, S.; Melikyan, A.; Kohl, M.; Koos, C.; Freude, W.; Dolores-Calzadilla, V.; Smit, M.; Suarez, I.; Martinez-Pastor, J.; Fitrakis, E. P.; Tomkos, I.; Optics and Photonics News vol. 24, pp. 28-35, 2013
- I. Suárez, E. P. Fitrakis, H. Gordillo, P. Rodríguez-Cantó, R. Abargues, I. Tomkos and J. Martínez-Pastor, Light Coupling from Active Polymer Layers to Hybrid Dielectric-Plasmonic Waveguides, Proceedings of the 14th International Conference on Transparent Optical Networks (ICTON 2013), 23-27 June 2013, Cartagena, Spain, IEEE Conf. Pubs., ISBN 978-1-4799-0682-6, pp. We.D6.3 - 1/4 (2013).
- Isaac Suárez, Henry Gordillo, Rafael Abargues, Pedro Javier Rodríguez-Cantó, Sandra Albert, Juan Martínez-Pastor, Dielectric and plasmonic waveguides based on quantum dots embedded in polymers, Opt. Pura Apl. 46 (4) 303-308 (2013)
- I. Suárez, E.P. Fitrakis, P. Geiregat, H. Gordillo, Y. Justo, P.J. Rodríguez-Cantó, Z. Hens, R. Abargues, D. Van Thourhout, I. Tomkos and J.P. Martínez-Pastor, SPP6, 2013, Ottawa, Canada, oral contribution.
- J. Leuthold, S. Muehlbrandt, A. Melikyan, M. Kohl, C. Koos, W. Freude, V. Dolores-Calzadilla, M. Smit, I. Suarez, J. Martínez-Pastor, E.P. Fitrakis and I. Tomkos, Plasmonic Communications: Light on a Wire, Optics & Photonics News, vol. 24, 28-35 (2013).

KIT

- 'Photonic-to-plasmonic mode converter' Melikyan, A.; Kohl, M.; Sommer, M.; Koos, C.; Freude, W.; Leuthold, J.; Optics Letters, Vol. 39, pp. 3488-3491, 2014
- 'High speed plasmonic phase modulators', Melikyan, A.; Alloatti, L.; Muslija, A.; Hillerkuss, D.; Schindler, P. C.; Li, J.; Palmer, R.; Korn, D.; Muehlbrandt, S.; Van Thourhout, D.; Chen, B.; Dinu, R.; Sommer, M.; Koos, C.; Kohl, M.; Freude, W.; Leuthold, J.; Nature Photonics, Vol. 8, pp. 229-233, 2014
- 'Plasmonic Communications: Light on a Wire', Leuthold, J.; Hoessbacher, C.; Muehlbrandt, S.; Melikyan, A.; Kohl, M.; Koos, C.; Freude, W.; Dolores-Calzadilla, V.; Smit, M.; Suarez, I.; Martinez-Pastor, J.; Fitrakis, E. P.; Tomkos, I.; Optics and Photonics News vol. 24, pp. 28-35, 2013
- 'Surface plasmon polariton absorption modulator' , Melikyan, A.; Lindenmann, N.; Walheim, S.; Leufke, P. M.; Ulrich, S.; Ye, J.; Vincze, P.; Hahn, H.; Schimmel, Th.; Koos, C.; Freude, W. and Leuthold, J.; Optics Express, Vol. 19, pp. 8855-8869, April 2011
- 'Fabrication of Ultra-Compact Plasmonic Waveguide Photo Diodes', Muehlbrandt, S.; Muslija, A.; Köhnle, K.; Melikyan, A.; Leuthold, J.; Kohl, M.; Micro and Nano Engineering (MNE'2014), Lausanne, Switzerland; Paper 8274.
- 'High-speed Plasmonic Modulators', Melikyan, A.; Alloatti, L.; Muslija, A.; Hillerkuss, D.; Schindler, P. C.; Li, J.; Palmer, R.; Korn, D.; Lindenmann, N.; Muehlbrandt, S.; Walheim, S.; Vincze, P.; Leufke, P. M.; Ulrich, S.; Ye, J.; Van Thourhout, D.; Chen, B.; Dinu, R.; Sommer, M.; Hahn, H.; Schimmel, Th.; Koos, C.; Kohl, M.; Freude, W.; Leuthold, J.; Advanced Photonics for Communications - Integrated Photonics Research, Silicon, and Nanophotonics (IPR'2014), San Diego (CA), Paper IT2A.6. [invited]

- 'Nonlinear Nano-Photonics', Freude, W.; Alloatti, L.; Korn, D.; Lauermann, M.; Melikyan A.; Palmer, R.; Pfeifle, J.; Schindler, P. C.; Weimann C.; Dinu, R.; Bolten, J.; Wahlbrink, T.; Waldow, M.; Walheim, S.; Leufke, P.; Ulrich, S.; Ye, J.; Vincze, P.; Hahn, H.; Yu, H.; Bogaerts, W.; Brasch, V.; Herr, T.; Holzwarth, R.; Hartinger, K.; Stamatiadis, C.; O'Keefe, M.; Stampoulidis, L.; Zimmermann, L.; Baets, R.; Schimmel, T.; Tomkos, I.; Petermann, K.; Kippenberg, T.J.; Koos, C. and Leuthold, J.; Optical Society of America 97th Annual Meeting (OSA'13): Frontiers in Optics (FiO'13), Orlando (FL), Paper FTu4C; USA, October 06–10, 2013
- 'Surface plasmon polariton high-speed modulator', Melikyan, A.; Alloatti, L.; Muslija, A.; Hillerkuss, D.; Schindler, P. C.; Li, J.; Palmer, R.; Korn, D.; Muehlbrandt, S.; Van Thourhout, D.; Chen, B.; Dinu, R.; Sommer, M.; Koos, C.; Kohl, M.; Freude, W.; Leuthold, J.; Conf. on Lasers and Electro-Optics (CLEO/IQEC'13), San Jose (CA), Paper CTh5D.2. [Postdeadline Paper]
- 'Ultracompact CMOS-compatible Modulators'. Leuthold, J.; Melikyan, A.; Korn, D.; Alloatti, L.; Palmer, R.; Koos, C.; Freude, W.; Proc. Frontiers in Optics Conference, OSA, Rochester, NY, paper FTu4A.1, Oct. 2012
- 'Chip-to-chip plasmonic interconnects and the activities of EU project NAVOLCHI', Melikyan, A.; Sommer, M.; Muslija, A.; Kohl, M.; Muehlbrandt, S.; Mishra, A.; Calzadilla, V.; Justo, Y.; Martinez-Pastor, J. P.; Tomkos, I.; Scandurra, A.; Van Tourhout, D.; Hens, Z.; Smit, M.; Freude, W.; Koos, C.; Leuthold, J.; 14th Intern. Conf. on Transparent Optical Networks (ICTON'12), University of Warwick, Coventry, UK, July 2–5, 2012 [NAVOLCHI, invited]
- 'Integrated wire grid polarizer and plasmonic polarization beam splitter' Melikyan, A.; Gaertner, C.; Köhnle, K.; Muslija, A.; Sommer, M.; Kohl, M.; Koos, C.; Freude, W.; Leuthold, J.; *Optical Fiber Communication Conference (OFC'12)*, Los Angeles (CA), USA, Paper OW1E.3 March 2012

TU/e

- M. Smit, E. Bente, V. Dolores-Calzadilla, and D. Heiss, “Lasers in generic photonic foundry platforms”, 24th International Semiconductor Laser Conference, plenary talk, 2014.
- V. M. Dolores Calzadilla, D. Heiss, and M. K. Smit, “Highly efficient metal grating coupler for membrane-based integrated photonics”, *Optics Letters*, 39(9), 2786-2789, 2014.
- V. M. Dolores-Calzadilla, A. Higuera-Rodriguez, D. Heiss, and M. Smit, “Efficient metal grating coupler for membrane-based integrated photonics”, *Integrated Photonics Research, Silicon and Nanophotonics (IPR) 2014*, IT2A.1, 2014.
- V. M. Dolores-Calzadilla, A. Millan-Mejia, J.J.G.M. van der Tol, and M. Smit, Diffraction-suppressed adiabatic tapers for photonic circuits, *Proceeding of the Proceedings of the 19th Annual Symposium of the IEEE Photonics Society Benelux Chapter*, 2014.

UVEG

- H. Gordillo, I. Suárez, R. Abargues, P. Rodríguez-Cantó and J.P. Martínez-Pastor, Color tuning and white light by dispersing CdSe, CdTe and CdS in PMMA nanocomposite waveguides, *IEEE Photon. J.* 5, 2201412 (12 pgs) (2013).
- J. Leuthold, S. Muehlbrandt, A. Melikyan, M. Kohl, C. Koos, W. Freude, V. Dolores-Calzadilla, M. Smit, I. Suarez, J. Martínez-Pastor, E.P. Fitrakis and I. Tomkos, Plasmonic Communications: Light on a Wire, *Optics & Photonics News*, vol. 24, 28-35 (2013).

- H. Gordillo, I. Suárez, R. Abargues, P. Rodríguez-Cantó, G. Almuneau and J. P. Martínez-Pastor, Quantum-dot double layer polymer waveguides by evanescent light coupling, *IEEE/OSA J. of Lightwave Technol.* 31, 2515-2525 (2013).
- I. Suárez, H. Gordillo, R. Abargues, P. Rodríguez-Cantó, S. Albert and J.P. Martínez-Pastor, Dielectric and plasmonic waveguides based on quantum dots embedded in polymers, *Opt. Pura Apl.* 46, 303-308 (2013).
- I. Suárez, A. Larrue, P.J. Rodríguez-Cantó, G. Almuneau, R. Abargues, V. S. Chirvony and J.P. Martínez-Pastor, Efficient excitation of photoluminescence in a two-dimensional waveguide consisting of a QD-polymer heterostructure, *Optics Letters* 39, 4692-4695 (2014).
- P. J. Rodríguez-Cantó; M. L. Martínez-Marco; R. Abargues ; V. Latorre-Garrido and J. P. Martínez-Pastor, Novel patternable and conducting metal-polymer nanocomposites: a step towards advanced multifunctional materials, *Proc. SPIE 8682, Advances in Resist Materials and Processing Technology XXX*, (9 pgs) (2013); <http://dx.doi.org/10.1117/12.2011716>.
- I. Suárez, E. P. Fitrakis, H. Gordillo, P. Rodríguez-Cantó, R. Abargues, I. Tomkos and J. Martínez-Pastor, Light Coupling from Active Polymer Layers to Hybrid Dielectric-Plasmonic Waveguides, *Proceedings of the 14th International Conference on Transparent Optical Networks (ICTON 2013)*, 23-27 June 2013, Cartagena, Spain, IEEE Conf. Pubs., ISBN 978-1-4799-0682-6, pp. We.D6.3 - 1/4 (2013).
- Isaac Suárez, Henry Gordillo, Rafael Abargues, Pedro Javier Rodríguez-Cantó, Sandra Albert, Juan Martínez-Pastor, Dielectric and plasmonic waveguides based on quantum dots embedded in polymers, *Opt. Pura Apl.* 46 (4) 303-308 (2013)
- I. Suárez, E.P. Fitrakis, P. Geiregat, H. Gordillo, Y. Justo, P.J. Rodríguez-Cantó, Z. Hens, R. Abargues, D. Van Thourhout, I. Tomkos and J.P. Martínez-Pastor, SPP6, 2013, Ottawa, Canada, oral contribution.
- R. Abargues, M. L. Martínez-Marco, P. J. Rodriguez-Cantó, J. Marques-Hueso, and J. P. Martínez-Pastor, Metal-polymer nanocomposite resist: a step towards in-situ nanopatterns metallization, *Advances in Resist Materials and Processing Technology XXX*, 25-27 February 2013, San José (USA), Oral contribution.
- P. J. Rodríguez-Cantó; M. L. Martínez-Marco; R. Abargues ; V. Latorre-Garrido and J. P. Martínez-Pastor, Novel patternable and conducting metal-polymer nanocomposites: a step towards advanced multifunctional materials, *Advances in Resist Materials and Processing Technology XXX*, 25-27 February 2013, San José (USA), Oral contribution.
- A. Maulu, P. J. Rodríguez-Cantó and J. P. Martínez-Pastor, Colloidal QD-solid photodetectors produced by doctor-blading based on two configurations: nano-gap (MIM) vs Schottky/heterostructure, 8th International Conference on Quantum Dots, 11-16 May, Pisa (Italy), Oral contribution.
- G. Muñoz-Matutano, D. Rivas, A. Ricchiuti, J. Bosch, D. Barrera, C. R. Fernández-Pousa, L. Seravalli, G. Trevisi, P. Frigeri, J. Martínez-Pastor and S. Sales, Exciton recombination dynamics of single InAs Quantum Dots emitting at long wavelengths, 8th International Conference on Quantum Dots, 11-16 May, Pisa (Italy), Poster.
- A. Maulu, P.J. Rodríguez-Cantó, I. Suarez, R. Abargues, J.P. Martinez-Pastor, "Fabrication of solution-processed QD-solids by doctor blading technique and their application for photodetection", 4th International Colloids Conference, 15-18 June, Madrid (Spain), Poster.
- I. Suárez, E. P. Fitrakis, R. Abargues, P. Rodriguez-Cantó, I. Tomkos and J. Martinez-Pastor, Photon plasmon coupling in nanocomposite plasmonic waveguides, 16th International Conference on Transparent Optical Networks (ICTON 2014) July 2014, Graz, Austria, oral (invited).

ETHZ

- C. Hoessbacher, Y. Fedoryshyn, A. Emboras, D. Hillerkuss, A. Melikyan, M. Kohl, M. Sommer, C. Hafner, and J. Leuthold, in CLEO: 2014(Optical Society of America, San Jose, California, 2014), p. FTu3K.6.
- C. Hoessbacher, Y. Fedoryshyn, A. Emboras, A. Melikyan, M. Kohl, D. Hillerkuss, et al., "The plasmonic memristor: a latching optical switch," *Optica*, vol. 1, pp. 198-202, 2014/10/20 2014.
- W. H. C. Haffner, Y. Fedoryshyn, D. L. Elder, A. Melikyan, B. Baeuerle, J. Niegemann, A. Emboras, A. Josten, F. Ducry, M. Kohl, L. R. Dalton, D. Hillerkuss, C. Hafner, and J. Leuthold. "High-Speed Plasmonic Mach-Zehnder Modulator in a Waveguide," presented at the ECOC, 2014.

Task 7.2 Exploitation

The main objective of this task is to explore the research outcomes of the NAVOLCHI project and promote market penetration of the end products. Due to the early stage of plasmonic technology, it is difficult to prepare for commercial products within or shortly after the timeframe of the project. At the same time, this early stage also means that project partners have the opportunity to lead the way in the technological advancement in their respective fields. In NAVOLCHI, this is mainly expressed through patent opportunities and innovative research through theses at the Master's and PhD level of participating institutions.

For a detailed list of exploitation activities, see D7.2. The main points are also summarized below.

- (UVEG) Patent: "Method to obtain metallic structures of nano- and micro-metric size from lithographic resists based on nanocomposites,, (P201201282).
(“Método de obtención de estructuras metálicas de tamaño nano y micrométrico a partir de resinas litográficas basadas en nanocomposites)
- V. M. Dolores-Calzadilla, A. Higuera Rodriguez, D. Heiss, (2014). “Metal grating coupler for membrane-based integrated photonics”, USA Provisional Patent Application filed, application number: 61/979, 2014.
- Theses (KIT, UGent, IMEC, UVEG):
 - (KIT) Calus Gaertner, “Plasmonic Modulators” (master thesis)
 - (UGent) Sukumar Rudra, “Diffractive Micro-Electromechanical Structures in Si and SiGe” (PhD Thesis).
 - (IMEC/UGent) Floris Taillieu, “Broadband colloidal quantum dot LED for active plasmonics” (master thesis).
 - (IMEC/UGent) Qi Lu, “Colloidal Nanocrystal Light Sources on Silicon”, (master thesis).
 - (UVEG) Henry Gordillo Millán, PhD thesis entitled “Guías ópticas activas de polímero con puntos cuánticos coloidales” (“Active optical waveguides based on polymers containing colloidal quantum dots”), 15th July 2013.
 - (UVEG) Mari Luz Martínez Marco, PhD thesis on conducting polymers containing metal nanoparticles and metal nano- and micro-structures using polymer-based patterns, under preparation.

- (UVEG) Víctor Latorre Garrido, “Propiedades Eléctricas y Ópticas del PMMA 3T-Au” (“Optical and electrical properties of PMMA-3T-Au”) (master thesis), December 2012.
- (UVEG) Alberto Maulu, PhD thesis on PbS quantum dot layers for developing photodetectors at telecom wavelengths (1st year).

Task 7.3 Promotion

Upcoming deliverables:

D7.5 Reports on the impact and outcome of organized promotion events (m36) – Moved to the end of the extension (M45).

D7.6 Final report on NAVOLCHI dissemination and promotion activities (m36) – Moved to the end of the extension (M45).

D7.7 Dissemination kit (m36) – Moved to the end of the extension (M45).

3.3 Project Management (Work Package 1)

3.3.1 Request for Amendment

As already explained in the intermediate report 2, the consortium requested for an amendment to the General Agreement to master the challenges raised by

- STs reduced engagement in work package 6, and
- Difficulties in the current tasks and with respect to STs reduced engagement.

Mainly, the amendment contained

- Adding ETH Zürich as a new partner to replace ST, and
- Extension of the project by 9 months.

Aside with topics of minor relevance, the amendment was granted by the EC at September 16th 2014. Major effects of this decision are discussed in 3.3.2 and 3.3.5. An updated Annex I to the General Agreement has been submitted to the EC by July 25th 2014.

3.3.2 Administrative Boards and Decisions

One consequence of the amendment is that Prof. Jürg Leuthold (ETH Zürich) becomes a member of the General Assembly instead of Alberto Scandurra (ST) and that he becomes work package leader of WP6.

General Assembly:

Karlsruhe Institute of Technology, Germany	KIT	Manfred Kohl
Interuniversity Microelectronics Centre VZW-IMEC, Belgium	IMEC	Dries Van Thourhout
Eindhoven University of Technology, Netherlands	TU/e	Meint Smit
Research and education laboratory in information technologies, Greece	AIT	Ioannis Tomkos
University of Valencia, Institute of Materials Science, Spain	UVEG	Juan Martinez Pastor
Eidgenössische Technische Hochschule Zürich, Switzerland	ETH	Jürg Leuthold
Ghent University, Belgium	Ugent	Zeger Hens

Table 1: General Assembly.

Technical Project Manager and Project Management Committee:

In June 2013, Prof. Jürg Leuthold (KIT/ETH Zurich) and Prof. Manfred Kohl (KIT) switched their positions in the Project Management Committee. Prof. Jürg Leuthold became Technical Project Manager, Prof. Manfred Kohl became Coordinator.

Technical Project Manager (Chair)		Jürg Leuthold
Coordinator		Manfred Kohl
+		
WP1 Leader	KIT	Manfred Kohl
WP2 Leader	AIT	Ioannis Tomkos
WP3 Leader	TU/e	Meint Smit
WP4 Leader	UVEG	Juan Martinez Pastor
WP5 Leader	IMEC	Dries Van Thourhout
WP6 Leader	ETH	Jürg Leuthold
WP7 Leader	AIT	Ioannis Tomkos

Table 2: Project Management Committee.

3.3.3 Management Deliverables

Deliverables covered by work package 1 with delivery dates are:

D1.1	Project web site with .eu domain (M01) and continuous update	11/2011
D1.2	Project reference online manual	01/2012
D1.3	Project quality assurance manual	04/2012
D1.4	Intermediate Progress Report 1	07/2012
D1.5	Intermediate Progress Report 2	04/2014

All have been prepared in time, for access to the WEB-site and the manuals please follow the links.

3.3.4 Communication: Meetings and Phone Conferences

Up to now, seven meetings and 30 phone conferences have been held:

Meetings:

- 1) Kick-Off meeting in Karlsruhe, Germany, February 3rd 2012.
- 2) Intermediate Meeting in Warwick, Great Britain, July 6th 2012.
- 3) Meeting in Ghent, Belgium, November 26th 2012.
- 4) Project Review Meeting 1 in Brussels, Belgium, November 27th 2012.
- 5) Midterm Meeting in Karlsruhe, Germany, April 26th 2013.
- 6) Project Review Meeting 2 in Brussels, Belgium, July 10th 2013.
- 7) Meeting in Eindhoven, Belgium, January 28th 2014.

To provide a short reaction time on possible problems, it was decided that phone conferences will be held every month if applicable, typically on the first Monday of every month.

Phone Conferences:

1) November 16 th , 2011	11) December 17 th , 2012	21) November 4 th , 2013
2) December 12 th , 2011	12) January 14 th , 2013	22) December 4 th , 2013
3) March 12 th , 2012	13) February 4 th , 2013	23) January 13 th , 2014
4) April 2 nd , 2012	14) March 4 th , 2013	24) March 3 rd , 2014
5) May 7 th , 2012	15) April 8 th , 2013	25) April 7 th , 2014
6) June 4 th , 2012	16) May 13 th , 2013	26) May 5 th , 2014
7) September 3 rd , 2012	17) June, 13 th , 2013	27) May 26 th , 2014
8) October 8 th , 2012	18) July 1 st , 2013	28) July 25 th , 2014
9) November 5 th , 2012	19) September 23 th , 2013	29) September 1 st , 2014
10) November 16 th , 2012	20) October 14 th , 2013	30) October 6 th , 2014

Detailed documentation of partner presentations, results obtained and decisions made during the meetings and phone conferences can be found in the minutes-files available on our [WEB-site](#) (please follow the link).

3.3.5 New Delivery Dates for Deliverables and Milestones

Deliverables and milestones with new delivery dates are listed below. A complete list can be found in the next subchapter.

D3.3	m24 → m33
D4.5	m33 → m42
D5.6	m30 → m39
D5.7	m33 → m42
D6.3, D6.4	m36 → m45
D7.5 - D7.7	m36 → m45

MS35, MS36, MS40	m30 → m39
MS41, MS42	m33 → m42
MS43, MS48, MS49	m36 → m45

3.3.6 Legal Status

No changes.

3.3.7 WEB-site

Since project start in November 2011, the WEB-site is available under www.navolchi.eu and is updated periodically. The WEB-Site is located at the Steinbuch Center for Computing (SCC), the IT- organization of the KIT, Karlsruhe.

3.3.8 Management Summary

As stated in the work package reports, most deliverables and milestones have been accomplished successfully, except the following:

- D2.5 and MS7 are late due to a lack of personnel resources.
- MS39 is completed in most instances but under continuous update. This seems to be useful in order to consider latest results from the new partner ETH. . A preliminary version can be presented on demand.
- D4.4 and MS24 will be delayed due to a number of technical reasons. D4.4 will be finished soon and MS24 needs to be shifted by 6 months.

Considering ETH as a new partner and the project extension by nine months, we are confident that these steps are appropriate to finish the outstanding tasks, especially in WP6, and to meet the remaining challenges of the project.

3.4 Deliverables and Milestones Tables

3.4.1 Deliverables

Status levels: finished in progress due critical

Deliverable		WP	Partner	Type	Diss	Delivery	
Nr.	Title					Mnth	Date
 D1.1	Project web site with .eu domain (M01) and continuous update	1	KIT	O	PU	1	11/2011
 D1.2	Project reference online manual	1	KIT	O	RE	3	01/2012
 D2.1	Definition of chip-to-chip interconnection system environment and specification	2	ST	R	RE	3	01/2012
 D1.3	Project quality assurance manual	1	KIT	O	RE	6	04/2012
 D5.1	DDCM specification document	5	ST	R	CO	6	04/2012
 D1.4	Intermediate progress report (1)	1	KIT	R	PU	9	07/2012
 D2.2	Definition of plasmonic devices	2	AIT	R	RE	12	10/2012
 D3.1	Report on studies of optimized structure for metallic / plasmonic nano-laser and its coupling to Si WG	3	TU/e	R	CO	12	10/2012
 D3.2	Report on modelling of the modulator structure	3	KIT	R	CO	12	10/2012
 D5.2	DDCM with electrical PHY design and verification data base	5	ST	R	CO	12	10/2012
 D4.1	Designs of plasmonic amplifiers	4	AIT	R	CO	18	04/2013
 D4.2	Report on optical properties of QDs layers and polymer nanocomposites	4	AIT	R	PU	18	04/2013
 D7.1	First report on NAVOLCHI dissemination and promotion activities	7	ST	R	RE	18	04/2013
 D7.2	First report on NAVOLCHI exploitation activities	7	AIT	R	RE	18	04/2013
 D7.3	Mirror Deliverable of D7.1, which will be available to the public on the website.	7	TU/e	R	PU	18	04/2013
 D7.4	Intermediate report on recent achievements.	7	AIT	R	PU	18	04/2013
 D5.3	Compact optical filters (2nm bandwidth, >30nm FSR) and first generation beam shapers	5	IMEC	R	CO	21	07/2013
 D2.3	Investigation of chip-to-chip interconnectionlevel specifications employing new plasmonic devices	2	AIT	R	RE	24	10/2013
 D2.4	Interface and plasmonic interconnect models and reports	2	ST	R	RE	24	10/2013

Table 3: Deliverables of the NAVOLCHI project, ordered by delivery date.

D3.4	Report on fabrication of modulators	3	KIT	R	CO	24	10/2013
D4.3	Designs of plasmonic photodetectors	4	AIT	R	CO	24	10/2013
D5.4	Generic DDCM compatible with plasmonic-based PHY specification document	5	ST	R	PU	24	10/2013
D5.5	Report on plasmonic waveguide couplers	5	KIT	R	CO	24	10/2013
D1.5	Intermediate progress report (2)	1	KIT	R	RE	27	01/2014
D6.1	Report on characterization results of all plasmonic devices	6	TU/e	R	RE	27	01/2014
D6.2	Report on characterization results of all optical interface plasmonic passive components	6	KIT	R	RE	27	01/2014
D2.5	Technoeconomical evaluation with respect to the cost efficiency and green aspects	2	AIT	R	PU	30	04/2014
D4.4	Report on SPP amplifiers by using QDs	4	IMEC	R	PU	30	04/2014
D3.3	Fabrication of plasmonic laser device	3	TU/e	R	CO	33	07/2014
D2.6	Report on new applications and their opportunities	2	AIT	R	PU	36	10/2014
D5.6	Generic DDCM compatible with plasmonic-based PHY design and verification data base	5	ST	R	CO	39	01/2015
D4.5	Report on plasmonic photodetectors	4	UVEG	R	PU	42	04/2015
D5.7	Second generation beam shapers (distance 1mm, with bandwidth > 10nm and efficiency > 3dB)	5	IMEC	P	CO	42	04/2015
D6.3	Report on chip to chip interconnect characterization	6	ST	R	PU	45	07/2015
D6.4	Report on plasmonic chip-to-chip interconnect prototype testing and evaluation	6	AIT	R	PU	45	07/2015
D7.5	Reports on the impact and outcome of the organized promotion events.	7	AIT	R	PU	45	07/2015
D7.6	Final report on NAVOLCHI dissemination and promotion activities	7	AIT	R	RE	45	07/2015
D7.7	Dissemination kit	7	AIT	O	PU	45	07/2015

Table 4: Deliverables of the NAVOLCHI project, ordered by delivery date (continued).

Diss: PU = Public

PP = Restricted to other programme participants (including the Commission Services).

RE = Restricted to a group specified by the consortium (including the Commission Services).

CO = Confidential, only for members of the consortium (including the Commission Services).

3.4.2 Milestones

Status levels: finished in progress due critical

Milestone		WP	Partner	Delivery	
Nr.	Title			Mnth	Date
 MS44	Dissemination of activities in the project's web site and continuous update	7	KIT	1	11/2011
 MS45	Press release on start of project to the public distributed	7	AIT	2	12/2011
 MS1	Definition of chip-to-chip interconnection system environment and specification	2	AIT	3	01/2012
 MS2	Definition of plasmonic devices and material properties for chip-to-chip interconnection	2	AIT	6	04/2012
 MS8	Decision on an optimized structure for metallic/plasmonic nano-laser and its coupling to Si waveguide	3	TU/e	6	04/2012
 MS9	Decision on an optimized structure for plasmonic modulator	3	KIT	6	04/2012
 MS25	Decision on optimized plasmonic waveguide couplers	5	KIT	6	04/2012
 MS10	Grown wafer structure for plasmonic lasers	3	IMEC	12	10/2012
 MS16	Decision on optimized structures for plasmonic amplifiers	4	UVEG	12	10/2012
 MS17	Synthesis of nanoparticles with gain at 1550nm	4	Ugent	12	10/2012
 MS26	Fabrication of plasmonic waveguide couplers with less than 3 dB coupling loss	5	KIT	12	10/2012
 MS27	Design of first generation beam shapers and compact optical filters	5	IMEC	12	10/2012
 MS28	DDCM with electrical PHY design and verification	5	ST	12	10/2012
 MS37	Plasmonic active device characterization results	6	KIT	12	10/2012
 MS11	Fabrication of plasmonic modulator on a SOI platform	3	KIT	15	01/2013
 MS18	Demonstration of conductive QD layers with photoconductive properties	4	UVEG	15	01/2013
 MS19	Demonstration of metal-(lithographic) polymer and QD metal-(lithographic) polymer nanocompo-sites	4	UVEG	15	01/2013
 MS29	Data codecs for power consumption reduction	5	ST	15	01/2013

Table 5: Milestones of the NAVOLCHI project, ordered by delivery date.

 MS30	Decision on plasmonic waveguide couplers with less than 3 dB coupling loss	5	KIT	15	01/2013
 MS46	Identification of possible contributions to the industrial partners for commercialization	7	ST	15	01/2013
 MS3	Development of a system and device simulation platform	2	AIT	18	04/2013
 MS4	Definition of the interconnection level specification employing developed plasmonic photonic devices	2	ST	18	04/2013
 MS12	Decision on an optimized structure for plasmonic modulator with a maximum loss of 20dB	3	KIT	18	04/2013
MS13*	Initial characterization of unbonded plasmonic lasers	3	TU/e	18	04/2013
 MS20	Demonstration and decision on photodetector operation: nano-gap (MIM) vs. Schottky / heterostructure	4	UVEG	18	04/2013
 MS21	Electroluminescence from QD stack embedded within conductive oxides (>1μW)	4	IMEC	18	04/2013
 MS31	Fabrication of compact optical filters and first generation beam shapers	5	IMEC	18	04/2013
 MS32	Data codecs for error detection and correction	5	ST	18	04/2013
 MS5	Digital domain to plasmonic domain interface specification and VHDL modelling	2	ST	21	07/2013
 MS14	Initial testing and characterization of plasmonic modulators	3	KIT	21	07/2013
 MS22	Demonstration of plasmonic amplifiers with optical pumping exhibiting 10dB gain  Appendix A	4	IMEC	21	07/2013
 MS6	Plasmonic interconnect VHDL modeling	2	ST	24	10/2013
 MS15	Initial testing of bonded plasmonic lasers	3	TU/e	24	10/2013
 MS23	Operation of QD based photodetector with responsivity > 0.1A/W	4	UVEG	24	10/2013
 MS33	Design of second generation beam shapers	5	IMEC	24	10/2013
 MS34	Generic DDCM compatible with plasmonic-based PHY	5	ST	24	10/2013

Table 6: Milestones of the NAVOLCHI project, ordered by delivery date (continued).

*) MS13 has been identified as inappropriate to the course of the project and was skipped in agreement with EC.

MS38	Plasmonic passive components characterization results with a 1dB coupling loss	6	KIT	24	10/2013
MS39	Concept for system integration developed	6	AIT	27	01/2014
MS7	Investigation of the cost and power consumption efficiency of the developed plasmonic devices	2	AIT	28	02/2014
MS24	Demonstration of SPP amplifiers with electrical injection exhibiting 10dB/cm gain	4	UVEG	30	04/2014
MS47	Organization of workshop on silicon photonics interface for chip-to-chip communication	7	TU/e	34	08/2014
MS35	Fabrication of compact optical filters and first generation beam shapers	5	IMEC	39	01/2015
MS36	DDCM evolution for NiP solutions	5	ST	39	01/2015
MS40	Individual plasmonic devices characterization, testing and evaluation	6	TU/e	39	01/2015
MS41	Chip to chip interconnect characterization	6	ST	42	04/2015
MS42	Plasmonic components integration to demonstrate chip-to-chip interconnect	6	AIT	42	04/2015
MS43	Plasmonic chip to chip interconnect prototype testing and evaluation	6	ST	45	07/2015
MS48	Public web site for NAVOLCHI prepared to stay open for at least another year	7	KIT	45	07/2015
MS49	Press release distributed comprising key results with a public target audience	7	AIT	45	07/2015

Table 7: Milestones of the NAVOLCHI project, ordered by delivery date (continued).

Comment to MS8: A suitable structure based on a plasmonic laser was designed, however further investigations are being carried out to design a metallic laser, which might offer a better performance.

4 Attachments

As determined in the projects “Description of Work”, the milestones (refer to chapter 3.4.2) achieved so far are delivered with this report. To avoid redundant lengthening of this document, the milestones are delivered as separate files. Additionally, you can find them on our web site www.navolchi.eu .